International Journal of Biological Macromolecules 253 (2023) 127409

Contents lists available at ScienceDirect

International Journal of Biological Macromolecules

journal homepage: www.elsevier.com/locate/ijbiomac

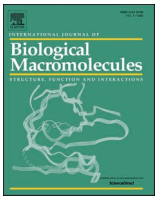

Paper as smart support for bioreceptor immobilization in electrochemical paper-based devices

Narjiss Seddaoui [a], Noemi Colozza [a,b], Ludovica Gullo [a], Fabiana Arduini [a,b,*]

[a] Department of Chemical Science and Technologies, University of Rome "Tor Vergata", Via della Ricerca Scientifica, 00133 Rome, Italy
[b] SENSE4MED S.R.L, Via Bitonto 139, 00133 Rome, Italy

ARTICLE INFO

Keywords:
Enzymes
Antibodies
Nucleic acids
Aptamers
Molecularly imprinted polymers

ABSTRACT

The use of paper as a smart support in the field of electrochemical sensors has been largely improved over the last 15 years, driven by its outstanding features such as foldability and porosity, which enable the design of reagent and equipment-free multi-analysis devices. Furthermore, the easy surface engineering of paper has been used to immobilize different bioreceptors, through physical adsorption, covalent bonding, and electrochemical polymerization, boosting the fine customization of the analytical performances of paper-based biosensors. In this review, we focused on the strategies to engineer the surface of the paper for the immobilization of (bio)recognition elements (eg., enzymes, antibodies, DNA, molecularly imprinted polymers) with the overriding goal to develop accurate and reliable paper-based electrochemical biosensors. Furthermore, we highlighted how to take advantage of paper for designing smart configurations by integrating different analytical processes in an eco-designed analytical tool, starting from the immobilization of the (bio)receptor and the reagents, through a designed sample flow along the device, until the analyte detection.

1. Introduction

The risk of health emergencies represents a main threat to human society that must be addressed in a framework of continuous growth of the population. The recent COVID-19 pandemic event highlighted the need for smart analytical tools with the overriding goal to help the management of health crises at a global scale. Miniaturized self-test devices are a key element to simplify the monitoring of disease spread helping in the identification of patients affected by the disease. Therefore, there is an urgent need to develop rapid and easy-to-use analytical tools, to face any future threat, whether biological or chemical.

In the era of sustainability, the design of rapid detection tools requires finding a compromise between technological progress and green aspects for delivering effective and eco-designed devices [1,2]. The green aspects embrace the principles of easy sample pre-treatment, miniaturized devices for on-site analysis, multiple analytes detection, reduction of the sample amount needed for the analysis, reduction of waste produced, and minimization of toxic reagents [3,4]. Considering the recent vision of White Analytical Chemistry, the cost-effectiveness, time efficiency, simplicity of procedures, and the reduction of advanced equipment/infrastructure are added features to evaluate for the development of environmentally friendly analytical tools [5].

The use of paper-based analytical devices (PADs) is increasing in the analytical field, as these devices meet many of the sustainability criteria such as the use of ubiquitous and renewable material like paper, cost-effectiveness, user-friendliness, low-energy, and plastic-free analysis [6–14].

Over the last 15 years, the paper has been used in several types of analytical tools. Whiteside group was the first to explore the development of PADs as colorimetric sensing devices, using PADs for the detection of glucose and protein in artificial urine [15]. In addition to colorimetric detection, paper has been introduced to electroanalysis in a pioneering study by C. S. Henry et al. in 2009 [16]. In that example, the filter paper was selected to realize screen-printed electrochemical cells, with higher sustainability with respect to the conventional supports used in screen-printing (e.g., plastic, ceramics). Moreover, the multiplex detection of glucose, lactate, and uric acid in human serum was achieved by driving the sample through microfluidic pathways defined on the paper by photolithography.

The work of Henry et al. awakened the researchers' attention toward the potentiality of PADs in the electrochemical field. Since then, considerable efforts have been made to develop PADs within all the

* Corresponding author at: Department of Chemical Science and Technologies, University of Rome "Tor Vergata", Via della Ricerca Scientifica, 00133 Rome, Italy.
E-mail address: fabiana.arduini@uniroma2.it (F. Arduini).

https://doi.org/10.1016/j.ijbiomac.2023.127409
Received 30 June 2023; Received in revised form 8 October 2023; Accepted 10 October 2023
Available online 15 October 2023

application fields and provide more practical and accurate eco-designed electroanalytical devices, demonstrating the effectiveness and versatility of PADs [16–18].

In this framework, an advantageous aspect relies on the use of paper for the immobilization of biocomponents by harnessing the porosity and the versatile chemistry of cellulose to entrap molecules within the cellulose matrix or to functionalize the paper itself for improving the immobilization efficiency.

The present review aims at describing and discussing the different strategies explored for the immobilization of biocomponents to develop electrochemical biosensors on paper supports. We believe that our review can provide an in-depth understanding of the benefits explored so far, furnishing the guidelines on how using the paper supports can deliver smart electrochemical biosensors that combine sustainability and relevant analytical performances.

In detail, our review initially provides a brief overview of the paper support involvement in the analytical field, highlighting the various characteristics that make the paper a leading alternative to conventional non-renewable materials. Then, a study of the various parameters that guide the selection of a specific type of paper is discussed, in combination with the right configuration (lateral or vertical flow). Finally, the main section of this review is devoted to a thorough study of how electrochemical PADs have been combined with different (bio)recognition elements (i.e., enzymes, antibodies, molecularly imprinted polymers, nucleic acids, aptamers, cells, peptides) for fabricating high-performance biosensing devices able to detect biological or chemical target analytes in different matrices including blood, urine, sweat, water, soil, and air.

2. Features of the paper for electrochemical (bio)sensing platforms

2.1. Paper properties for (bio)sensing

Paper has been used for chemical measurements for centuries, starting from litmus paper used to measure pH in 1784 [19]. Since the works of Whiteside and Henry's groups, PADs have been increasingly used for the development of colorimetric and electrochemical sensing devices. A search of the Scopus database using the sentence "paper-based analytical device" yields more than 1500 scientific papers demonstrating several works on developing paper-based devices.

The widespread use of paper as a solid support in the manufacture of PADs can be attributed to its outstanding characteristics [7,13,20,21]. Table 1 summarizes the main properties that make the paper an irreplaceable material for electrochemical (bio)sensor development.

Considering the sustainability, i) the production and disposal of cellulose itself are more sustainable processes when compared to other materials for sensor development (e.g., ceramic, plastic), ii) few microliters (e.g., 5, 10 μL) are commonly required for PAD preparation (e.g., loading of reagents) minimizing the amount of reagents, and iii) the waste resulting from the analysis is minimal both in terms of reagents used and sample required, bringing advantages in the sampling procedure as well as the waste disposal. Furthermore, the paper itself can be disposed of by incineration, further reducing the impact of waste production and management.

Table 1
Summary of the most significant paper properties in the development of PAD-based (bio)sensors.

Environmental sustainability	Economical and practical advantages	Key features for customizable applicability
• Sustainable sources • Easy disposability • Minimization of the reagents • Minimization of the waste	• Worldwide availability • Lightness • Affordability • Easy/ready-to-use devices • Screening analysis	• Easy cut and folding • Biocompatibility • Porosity • Capillary forces • Adsorption properties

Considering the technical aspect, paper can be easily cut and folded, allowing for the realization of a variety of sensor configurations. In addition to the simplest configuration, e.g., a single piece of paper used as the support for electrode deposition, complex structures can be designed using origami configuration.

Additionally, the hydrophilicity nature and the porous structure of cellulose allow the liquids (e.g., reagents, samples) to flow through the paper matrix, driven by capillary action without the need for external forces. This feature makes PAD-based (bio)sensors standalone devices and offers advantages for on-site applications (e.g., avoiding the use of external pumps and improving the overall portability and easiness of use).

The porosity of the paper enables also the easy storage of the reagents. Typically, a few μL of the reagents needed for the analysis are loaded on the porous paper, being immobilized through van der Waals interactions, hydrogen bonds, or specific covalent modifications (i.e., surface engineering). This approach is suitable for producing reagent-free PAD-based (bio)sensors, which are ready for the analysis of the target analyte without the need for additional reagents.

2.2. Types of paper supports used in the development of (bio)sensing platforms

Different types of papers can be employed for the design of (bio) sensing devices, enabling the device to be customized for the selected application. The most widely used renewable materials like filter paper, blotting paper, glossy paper, office paper, and nitrocellulose (NC) membranes are manufactured from cellulose-supports such as wood or cotton by compressing and treating the cellulosic fibers [22–24]. The use of cellulose in the manufacture of PADs not only helps to preserve the environment from polluting waste materials, but cellulose itself possesses a large number of hydroxyl groups that can be functionalized to further improve its characteristics, e.g., by the addition of surfactants, polymers, aldehydes or epoxy groups [25–27].

In general, the main parameters to consider when selecting a specific type of paper among others are the porosity, thickness, retention capacity, flow rate, weight, functional groups, and brightness, which differ widely from one type to another. For instance, filter paper is the most commonly used material in PAD construction due to its wicking capabilities, uniform thickness, retention capacity, and high reagent absorption. Among commercially available papers suitable for filtration, Whatman grade 1 filter paper is known for its high wicking capacity and low pores size (~11 μm) at the same time [28]. This grade of filter paper is composed of about 98 % cellulose and provides a uniform and smooth surface with a thickness of 180 μm, in addition to moderate retention and flow velocity. In contrast, Whatman grade 4 filter paper, which has larger pores (~25 μm), is preferred when a higher liquid retention rate is required [29].

NC membranes belong to the second type among the most used cellulose supports, especially in the development of lateral flow assays (LFAs) due to their higher protein binding capacity. This type of membrane can be produced by partial nitration of cellulose in the presence of nitric acid [30]. The nitration process introduces functional groups to the cellulose, enabling the covalent immobilization of biomolecules (e.g., enzymes, antibodies, DNA) through the strong dipoles of the nitrate groups or by electrostatic adsorption between the positively charged biomolecules and the negatively charged NC membranes surface [31]. Although NC membranes have a uniform pore size (0.45 μm), high retention rate, and smooth surfaces, they are more mechanically fragile than filter paper and are not suitable for wax printing. In general, there are three main types of NC membranes used in biosensing, especially in point-of-care testing (POCT): HF-90, HF-135, and HF-180. The porosities and pore sizes of HF-90, HF-135, and HF-180 are 80.65 %, 79.54 %, and 78.67 % and 10–55 μm, 10–30 μm, and 9–14 μm, respectively [30].

In addition to the above-mentioned materials, other types of paper with special properties have been used for the preparation of PADs, including paper activated by functional groups such as carboxyl groups suitable for enzyme immobilization [32], office paper being cheap and readily available paper on the market, characterized by its mechanical strength and smooth surface [33], and glossy paper for its hydrophobic nature used because easily engineered [34]. In Table 2, a brief presentation of the main properties defining the paper types most commonly used in PAD fabrication is provided.

It is not surprising that the selection of the type of paper is a crucial step that likely determines the characteristics of the resulting electrochemical PAD. The first parameter to be considered is the hydrophilic/hydrophobic nature of the support, which dictates the possibility of using organic solvents or aqueous solutions during the sensing application. Another relevant parameter is the strength of the material: more robust paper types are more suitable for easier handling, reducing the risk of mechanical degradation during the PAD utilization. For instance, filter paper and office paper can be used as robust supports for the screen-printing of conductive inks to produce printed electrochemical cells. The robustness of the paper can also be improved by applying wax layers, which is one of the most used approaches for patterning microfluidic pathways on paper. Porosity is another important factor to be considered in relation to the final application of the PAD because i) the pore size within the cellulose matrix has a direct impact on the filtration or pre-concentration processes that occur during the PAD preparation or application, ii) porous papers can enable the simple drop-cast of the biocomponent (as well as any other needed reagents) to be entrapped within the matrix pores.

Table 2
Main properties of different paper types used for the construction of PAD-based (bio)sensors.

Paper type	Physical properties	Chemical properties	Availability (cost)
Whatman grade 1 filter paper	• Pores size (~11 μm) • Low adsorption ability • High mechanical strength • High biodegradability	• Hydrophilicity • Made of 98 % of cellulose • Abundant hydroxyl groups (-OH)	Low cost
Whatman grade 4 filter paper	• Pores size (~25 μm) • Low adsorption ability • High mechanical strength • High biodegradability	• Hydrophilicity • Made of 98 % of cellulose • Abundant hydroxyl groups (-OH)	Low cost
Nitrocellulose membrane	• Pores size (~9–55 μm) • Excellent adsorption ability • Weak mechanical strength • Excellent biocompatibility	• Hydrophobicity • Presents strong dipoles of nitrate groups	Expensive
Office paper	• Pores size (~10 μm) • Low adsorption ability • High mechanical strength	• Relative hydrophobicity • Composed of cellulose and alkyl ketene dimer	Cheap
Glossy paper	• Weak adsorption ability • High mechanical strength • Non degradable • High brightness and whiteness	• High hydrophobicity • Made of cellulosic fibers bonded to inorganic fillers	Cheap

2.3. Configurations of paper-based analytical devices

After selecting the most suitable paper type, the designing of the configuration of the PADs is another fundamental step. The configuration combines specific properties of the selected paper type with additional features that can be obtained from the folding, cutting, and overlapping of different layers of paper. Microfluidics PADs can be designed in a two-dimensional (2D) configuration, in which the liquid moves horizontally across the paper, or in three-dimensional (3D) structures, in which the liquid moves vertically across the paper, by exploiting also the folding and/or the overlapping of different paper layers.

These patterns are typically designed using chemical methods such as photolithography, wax printing, inkjet printing, laser printing, flexographic printing, stamping, chemical vapor deposition, screen-printing, and spraying [35], or by using physical methods such as knife plotting, craft cutting, embossing, and laser cutting [36].

The 3D configuration seems more interesting in terms of improving the performances of (bio)sensors, as it allows for multi-step testing using multiple layers of paper. Each layer can be designed as responsible for a specific chemical reaction and then transfer the corresponding product to the next layer [37]. Typically, the paper layers are overlapped through two main strategies to fabricate 3D devices: i) by stacking different paper layers, e.g., via a double-sided adhesive or using a glue [38], which allows for using different types of papers in the same device, and ii) by folding a single piece of 2D patterned paper to obtain a 3D structure, obtaining an origami-like configuration [12]. In such a format, the fluid is driven perpendicularly to the paper surface (i.e., vertical flow), however, more sophisticated structures are additionally designed to exploit both lateral and vertical flow across the paper layers.

The employment of properly selected paper types and a customized design in 2D or 3D configuration (with vertical/lateral flow), has paved the way for a new generation of plastic-free electrochemical (bio)sensors. The following sections are devoted to a critical discussion of the most relevant examples of paper-based electrochemical biosensors reported in the literature. In detail, the discussion is organized to highlight how different paper types and their properties can be efficiently exploited to immobilize the (bio)components on the paper matrix, by taking advantage of the multifunctional properties of the paper itself.

3. (Bio)recognition elements for electrochemical PADs preparation

3.1. Enzymes

As highlighted earlier, the first electrochemical PAD was designed by Henry's group in 2009, for simultaneously detecting glucose, lactate, and uric acid in serum samples using GOx, lactate oxidase, and uricase, respectively [16]. As depicted in Fig. 1A, the oxidase enzymes were simply cast on the three different working electrodes (WE). Each WE was printed with carbon ink containing Prussian blue, which electrochemically mediates the reduction of hydrogen peroxide, as the enzymatic by-product. The biosensors showed promising analytical performances, with a limit of detection (LOD) of 0.21 mM, 0.36 mM, and 1.38 mM, for glucose, lactate, and uric acid, respectively.

Since then, enzymes pre-loading on paper supports by a simple drop-casting method has become one of the most widely used methods for the preparation of enzymatic PADs, because it is easy to fabricate, inexpensive, requires only a few microliters of an enzyme, preserves the integrity of the enzyme, and does not affect the chemical resistance of the paper support.

An additional example of enzymatic paper-based biosensors is reported by Li et al. who developed a sandwich-type origami PAD using Whatman chromatographic paper (grade 1) to detect glucose in human blood samples [39]. This configuration comprises two separate pads: an enzymatic zone to load the GOx, and a second pad that works as an

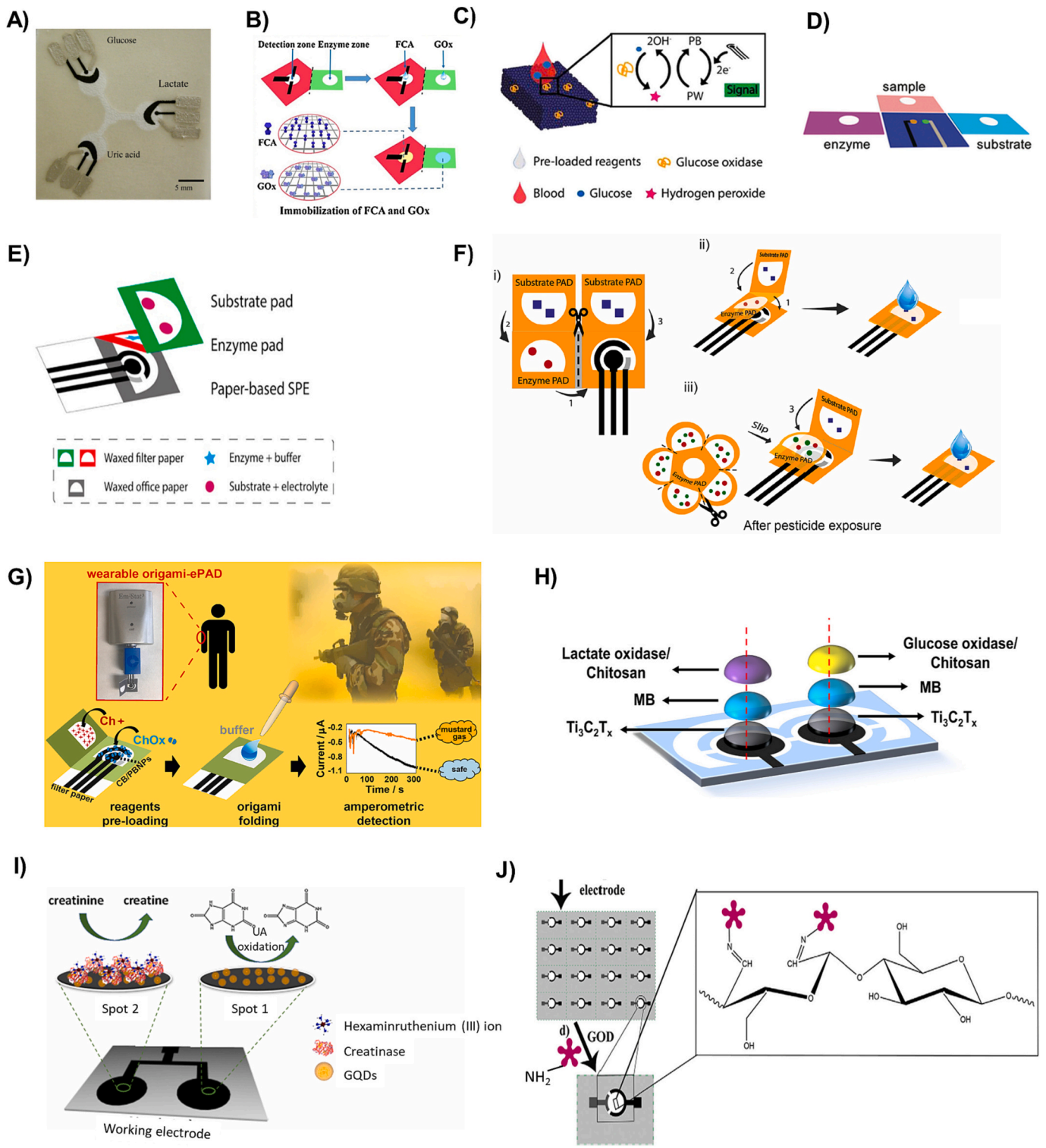

Fig. 1. A) Paper-based microfluidic enzymatic biosensor for simultaneous detection of glucose, lactase, and uric acid. Reprinted with permission from [16], 2009 ACS Publications. B) Fully drawn origami paper analytical device for electrochemical detection of glucose. Reprinted with permission from [39], 2016 Elsevier. C) Paper-based biosensor for glucose detection in whole blood based on the synthesis of Prussian Blue Nanoparticles in the paper. Reprinted with permission from [41], 2018 Elsevier. D) An origami paper-based device for potentiometric biosensing. Reprinted with permission from [47], 2016 Wiley Online Library. E) An origami paper-based electrochemical biosensor for pesticide detection. Reprinted with permission from [48], 2019 Elsevier. F) A paper-based electrochemical device for the detection of pesticides in aerosol the phase. Reprinted with permission from [49], 2022 Elsevier. G) A wearable origami paper-based electrochemical biosensor for sulfur mustard detection. Reprinted with permission from [50], 2019 Elsevier. H) A paper-based sensor for wearable electrochemical sweat analysis. Reprinted with permission from [53], 2021 Elsevier. I) A microfluidic electrochemical paper-based device for the simultaneous determination of clinical biomarkers. Reprinted with permission from [56], 2019 Elsevier. J) A 3D paper-based microfluidic electrochemical glucose biosensor based on rGO-TEPA/PB sensitive film. Reprinted with permission from [57], 2019 Elsevier.

electrochemical cell containing pencil-drawn WE modified with the electrochemical mediator ferrocenecarboxylic acid, as shown in Fig. 1B. To conduct the analysis, the device was folded along a central hole to bring the electrodes into contact with the enzymatic pad, followed by the addition of the sample. The linear range and the detection limit obtained with the developed PAD were 1–12 mM and 0.05 mM, respectively.

The sandwich-type origami configuration was also used by Liang et al. for the determination of glucose in the presence of electrochemical interferents such as urate, ascorbate, and paracetamol [40]. The drop-casting strategy was used to load GOx onto the cover layer of a two-zone enzymatic pad, which was placed over conventional screen-printed electrodes. To selectively detect glucose, sample was added to the electrochemical cell to completely consume urate, ascorbate, and paracetamol by electrolysis with an applied potential of +0.7 V (vs. Ag/AgCl RE), then the enzymatic pad was folded onto the WE and GOx was dissolved in the electrolyte solution, enabling the coulometric detection of glucose in the range of 0–24 mM with recoveries comprised between 98 and 102 %.

Our group has immobilized GOx onto a home-made "Paper Blue" support. The as called "Paper Blue" was obtained by soaking filter paper with Prussian blue precursors (i.e., potassium ferricyanide ($K_3Fe(CN)_6$) and iron chloride ($FeCl_3$)) that were then reduced on the paper network to form PBNPs because of the presence of impurities in the cellulose matrix [41]. The as-prepared "Paper Blue" was employed as a support to print the electrochemical cell by the screen-printing method. To deliver a reagents-free PAD, the WE was preloaded with a few microliters of GOx and finally used for the amperometric determination of glucose in the analytical range comprised between 0 and 30 mM, as shown in Fig. 1C. The eco-designed "Paper Blue" served in this study as both a reservoir for GOx preloading and a reactor for PBNP synthesis, thus providing an all-in-one biosensor that is straightforward to use by non-specialists. In addition, the "Paper Blue" demonstrated a very satisfactory correlation coefficient of 0.987 with commercial glucose strips (Bayer Contour XT), demonstrating its practicability in glucose monitoring.

In another approach, filter paper was used as a reservoir for loading GOx, thereby delivering a paper-card-like that can be inserted into an in-house made polyvinyl chloride (PVC) electrochemical cell [42]. Herein, the Prussian blue mediator was not reduced on the paper network but instead was loaded onto a working zone delimited on a strip of filter paper using a wax patterning method. In detail, PBNPs were previously synthesized in an acidic solution in the presence of carbon black (CB), obtaining a dispersion of CB decorated with PBNPs. This strategy has been thoroughly explored by our group [43,44], taking advantage of using CB for improving the stability of PBNP dispersion. The CB/PBNPs nanocomposite modified sensing area was preloaded with a few microliters of GOx before being inserted into the PVC-based electrochemical cell holding the gold, silver, and copper as the working, reference, and counter electrodes, respectively. The combination of the GOx-modified pad and the PVC cell allows for the reuse of the electrochemical cell by simply inserting a new pad for each assay, thus helping to minimize waste production and costs. The paper card-like electrochemical platform was successfully applied for the detection of glucose in artificial tears within the range of 0.2–2 mM with a detection limit of 50 μM.

Another well-known family of enzyme biosensors is based on the cholinesterase enzyme. This enzyme presents a high turnover rate and it is used for the detection of target analytes such as organophosphate pesticides and nerve agents, having inhibition capability towards this enzyme. Using this sensing principle, butyrylcholinesterase (BChE) has been selected as a bioreceptor for the quantification of paraoxon, a nerve agent simulant. BChE hydrolyzes the butyrylthiocholine into an electroactive by-product, thiocholine, which can be detected in the amperometric mode (e.g., +0.3 V vs. Ag/AgCl RE). Paraoxon is able to irreversibly inhibit BChE activity, thus BChE inhibitive biosensors reveal paraoxon presence. To prepare a one-shot PAD, our group merged in one platform NC membrane impregnated with butyrylthiocholine and a filter paper holding an electrochemical cell printed on a waxed-paper test area, pre-loaded with BChE. After incubating BChE with paraoxon solution for 10 min, a detection limit as low as 3 μg/L was obtained. The prepared biosensor was successively applied to analyse paraoxon in untreated river water and wastewater samples with recoveries of 89 ± 8 % and 92 ± 8 %, respectively, confirming its usefulness for environmental surveillance [45].

To reduce the number of paper layers used, Cioffi et al. modified office paper-based screen-printed electrodes with the same components involved in the previous work, by casting a mixture of PB, CB, and BChE onto the WE in a single drop [46]. The biosensor built on a single layer of office paper enabled the detection of 1.3 ng/mL paraoxon in buffer solutions under an applied potential of +0.2 V (vs. Ag/AgCl RE). However, the system requires the addition of the enzymatic substrate during the electrochemical analysis, hindering the design of a reagent-free device. Soil and vegetable samples were also analyzed, and good recovery values (i.e., 84–103 %) were calculated.

BChE was also used in a 3D origami setup for the development of a potentiometric ion-sensing PAD, which was designed for detecting the choline cation generated by the enzymatic hydrolysis of butyrylcholine [47]. To ensure selective control of butyrylcholinesterase activity in the presence of methyl parathion, an organophosphate pesticide, heptakis (2,3,6-tri-*o*-methyl)-b-cyclodextrin was used as an ionophore. The 3D origami biosensor consists of a test pad bordered by three folding pads for loading BChE (enzyme pad), butyrylcholine (substrate pad), and the sample to be analyzed (sample pad), as shown in Fig. 1D. To perform potentiometric measurements, the test pad was cast with few drops of carbon and Ag/AgCl inks to create a working and a reference electrode, respectively. After folding the sample pad with the enzyme pad for 5 min, the sample pad was unfolded and the enzyme pad was refolded with the substrate pad, with the addition of a few μL of running buffer, to determine the degree of inhibition of BChE by methyl parathion. With this ready-to-use PAD, a dynamic range between 0.1 and 1.0 nM was observed, allowing for the detection of methyl parathion at the nanomolar level.

For more practical use, a 3D origami PAD device was fabricated by our group for the simultaneous detection of paraoxon, 2,4-dichlorophenoxyacetic acid, and atrazine by exploiting the ability of these pesticides to inhibit BChE, alkaline phosphatase (AP), and tyrosinase, respectively [48]. This device was designed by integrating office paper-based screen-printed electrodes and various foldable filter paper-based pads that were used to load the enzymes and their corresponding substrates, as demonstrated in Fig. 1E. For each pesticide, two enzyme foldable pads and two substrate foldable pads were used to monitor the enzymatic activity of the corresponding enzyme in the absence and presence of the inhibitor. The analysis required the addition of a few μL of distilled water on the first couple of PADs which are then put into contact with the printed electrode for the detection of enzymatic activity in the absence of the inhibitor, consequently, this couple of PADs is cut. Afterward, a few μL of pesticide samples are added to the enzyme pad of the second couple of PADs, which is then folded after 5 min together with the substrate pad onto the WE, and the measurement was carried out by adding a few μL of distilled water. By performing chronoamperometric analysis, all three pesticides were detected at ppb level in the standard solutions and in the river water sample with satisfactory recoveries (80–93 %).

Our group later developed a flower-like PAD inspired by nature for the detection of paraoxon, 2,4-dichlorophenoxyacetic acid, and glyphosate in the aerosol phase, by monitoring their inhibition effects on BChE, AP, and peroxidase activities, respectively [49]. In contrast to the previous design, the present PADs consist of a flower-like pad consisting of enzyme-preloaded petals that will be exposed to the pesticide-charged aerosols and then slid onto the electrochemical cell for inhibitor determination (Fig. 1F). By conducting amperometric measurements, these

novel PADs were able to detect three classes of pesticides in the aerosol phase with limits of detection equal to 30 ppb, 10 ppb, and 2 ppb for 2,4-dichlorophenoxyacetic acid, glyphosate, and paraoxon, respectively.

In addition to nerve agents, the development of PADs based on enzyme inhibition was applied in the security field for the monitoring of other hazardous agents. Our group reported the fabrication of a wearable origami-type electrochemical PAD for the detection of aerosol-phase sulfur mustard agent, a chemical warfare agent that has been widely used in the first half of the 20th Century [50]. The sensing principle was based on the ability of mustard gas to inhibit the enzymatic activity of the choline oxidase enzyme (ChOx). In this case, the filter paper was chosen as a porous material to immobilize a few microliters (i.e., 5 μL) of the reagents by simple drop-casting, followed by a drying step. To realize such a design, the filter paper was printed with three electrochemical electrodes in which a conductive graphite ink containing a CB/PBNP nanocomposite was used to print the WE and the CE. The ChOx enzyme was then loaded onto the same hydrophilic area of the WE, while the substrate (choline) was loaded on another foldable filter pad, as illustrated in Fig. 1G**.** The enzyme was allowed to react with the substrate by folding the pads and exposing the biosensor to both a liquid or aerosol sample, obtaining an inhibition in the presence of mustard agents (i.e., bis-(2-chloroethyl)-amine) that was monitored in chronoamperometry at +0.0 V (vs. Ag/AgCl RE). This biosensor was applied for real-time detection of sulfur mustard, obtaining limits of detection equal to 1 mM and 0.019 g/m^3 for liquid and aerosol phases, respectively.

Physical adsorption was found to be effective in immobilizing 3-hydroxybutyrate dehydrogenase (3-HBHD) on chromatographic paper (grade 1) for the preparation of a "pop-up" electrochemical PAD measuring beta-hydroxybutyrate (BHB), a biomarker for diabetic ketoacidosis, using a commercial glucometer [51]. The pop-up PAD includes a sample pad (port pad) and a reaction zone preloaded with 3-HBHD (enzyme pad), designed separately from a detection area (detection pad) that includes three stencil-printed electrodes used to connect the pop-up PAD to a glucometer. Blood samples were introduced onto the sample pad in open mode, and after 2 min of the enzymatic reaction, the pop-up PAD was folded to bring the enzyme pad into contact with the detection pad. Folding/unfolding the pop-up structure allows for easy modification of the flow path, control of the valve and timing, and reconnection of the layers in the pop-up structure space. The pop-up PAD showed a good linear fit in the clinically relevant range of 0.1 to 6.0 mM ($R^2 = 0.96$) with a detection limit equal to 0.3 mM.

Still with the physical adsorption, phenylalanine dehydrogenase enzyme (PheDH) was immobilized on filter paper-based microzones coupled to screen-printed carbon electrodes for the electrochemical detection of phenylalanine (Phe), an indicator of dysfunctional amino acid metabolism [52]. Here, paper microzones delimited with wax were loaded with PheDH by a drop-casting method and allowed to dry before being placed on the electrochemical electrode previously modified with reduced graphene oxide (rGO) that was used to boost the electrochemical performance of the prepared PAD. PheDH in the presence of NAD^+ catalyzes the reversible deamination of Phe to form phenylpyruvate, ammonia, and NADH. The latter can be monitored by differential pulse amperometry (DPA) at +0.6 V (vs. Ag/AgCl RE) harnessing the ability of rGO to promote electron transfer with NADH. The responses obtained with the prepared microzone-based PAD were linear in the range comprised between 1 and 600 μM, resulting in a LOQ of 1 μM and LOD of 0.2 μM.

Although physical adsorption is a very simple and fast method, one of the main drawbacks relies on the leaching of enzymes from the PAD into the reaction media.

To face this issue, a polymer like chitosan was selected as a biocompatible polymer to confine enzymes (e.g., GOx and lactate oxidase) into a stable network [53]. For instance, Wang et al. [53] developed a bi-enzymatic PAD for the detection of glucose and lactate in sweat by immobilizing GOx and lactate oxidase through a few drops of chitosan solution cast onto the selected working electrodes (Fig. 1H). Owing to the vertical path diffusion, sweat samples can be efficiently collected and rapidly diffused toward the working electrodes. The developed origami PAD displayed a dynamic range between 0.08 and 1.25 mM with a detection limit of 17.05 μM in the case of the glucose biosensor, and within the range of 0.3–20.3 mM with a detection limit of 3.73 μM in the case of the lactate biosensor, thus demonstrating its sufficient merits to be used for real-time sweat analysis.

In another work, the ability of chitosan to form stable aqueous dispersions of carbon-based nanomaterials (e.g., carbon black) was exploited to immobilize GOx on sixteen independent working areas designed on Whatman filter paper (Grade 1) for high-throughput multiplexed analysis of glucose in urine samples [54]. The preparation of this multiple microfluidic system was achieved by using a laser printer to produce the microfluidic pattern combined with 16 polyester-based electrodes for multi-analysis. The working electrodes were modified with a few drops of enzymatic mixture obtained by adding GOx to a dispersion of chitosan and CB nanoparticles for hydrogen peroxide detection at +0.6 V (vs. Ag/AgCl RE). Upon addition of samples to the sample chamber located in the center of the electrochemical system, glucose flows by capillary forces to the working electrodes on which it can be quantified in 16 replicates. The calibration curve obtained by the present device was linear in the analytical range between 1.0×10^{-4} M and 4×10^{-2} M, with a detection limit equal to 3×10^{-5} M.

The successful integration of chitosan in the preparation of enzyme-based PADs can be attributed to its excellent features such as biocompatibility, biodegradability, absorption capacity, and, above all, the abundance of reactive groups, namely the primary amino group and the primary and secondary hydroxyl groups, which can be used for covalent bonds or, if charged, for electrostatic interactions with enzymes [55].

Another way to immobilize enzymes on the paper support is to exploit the high surface-to-volume ratio of nanomaterials. Cincotto et al. synthesized nanocrystalline particles of graphene quantum dots (GQDs) and used them for the immobilization of creatininase [56]. The microfluidic PAD consists of two spot sensors designed on the same working electrode for the simultaneous determination of uric acid and creatinine in human urine samples, as depicted in Fig. 1I. The first spot was modified with only GQDs for direct oxidation of uric acid, while the second spot was coated with a few μL of GQDs, followed by the addition of the enzyme mixture consisting of creatininase and glutaraldehyde. Glutaraldehyde was additionally used as a cross-linking reagent. The manufacture of the present PAD involved sandwiching a filter paper-based microfluidic channel (sample pad) between two polyester sheets used for printing the electrochemical cell. By applying the sample to the injection area, simultaneous determination of uric acid and creatinine was achieved in the range 0.010–3.0 μM, with detection limits equal to 8.4 nM and 3.7 nM for uric acid and creatinine, respectively.

Taking advantage of the presence of abundant polyol functional groups on filter paper, the periodate oxidation method was used to create an aldehyde-functionalized hydrophilic zone for covalent attachment to the amino group ($-NH_2$) of GOx [57]. In detail, covalent immobilization of GOx to the hydrophilic zone was accomplished in two steps: (i) periodate oxidation of the cellulose hydroxyl groups, which involves opening glycosidic rings by cleaving the carbon-carbon bond of a vicinal diol, leaving two pendant aldehyde groups, and (ii) imine formation between the aldehyde group and the amino group of GOx, as shown in Fig. 1J**.** To this end, GOx was dropped onto the hydrophilic area of the CE/RE layer previously soaked for 2 h in a potassium periodate solution (KIO_4) to introduce the aldehyde groups of the filter paper surface. After stacking the two layers, the 3D paper-based microfluidic device was applied to the determination of glucose and it showed a wide linear range between 0.1 mM and 25 mM, with a detection limit of 25 μM.

3.2. Antibodies

Antibodies constitute another class of biorecognition elements widely employed for PAD preparation. These bioreceptors have been integrated for many years into immunochromatographic assays, which are one of the simplest, most affordable, and fastest immunoassays to fabricate [58]. However, to overcome one of the main drawbacks of LFAs, namely their lack of sensitivity, considerable efforts have been devoted to the efficient integration of LFA strips into electrochemical assays, which ensure rapid and sensitive sample analysis. In addition, electrochemical analyses require a very small amount/volume of sample that may not require any pretreatment steps. Depending on several factors (eg., paper type, PAD configuration), antibodies can be immobilized on a paper support through physical adsorption (by dispensing a

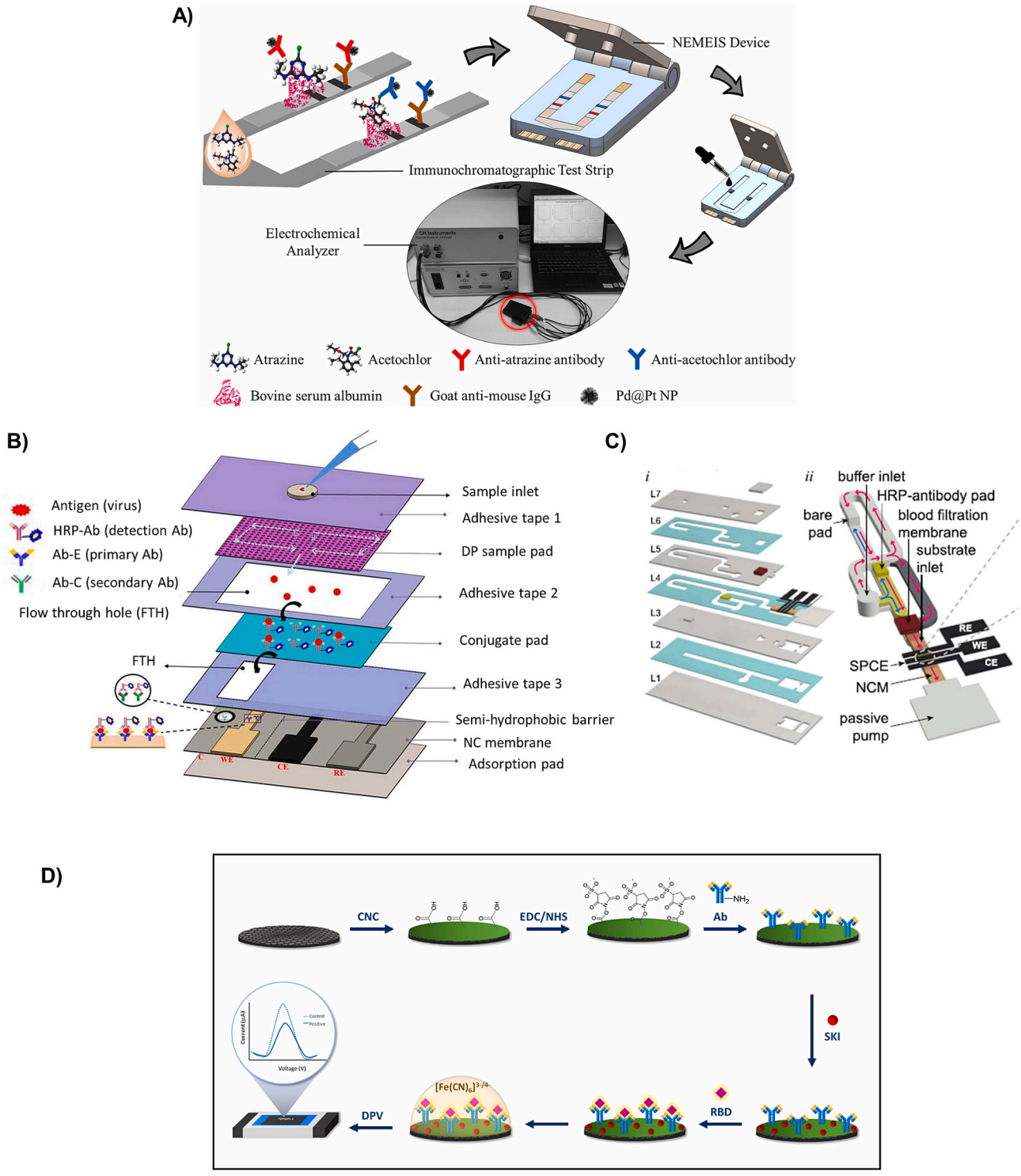

Fig. 2. A) A 3D-printed sensor platform for simultaneous detection of atrazine and acetochlor. Reprinted with permission from [59], 2021 Elsevier. B) A vertical flow-based paper immunosensor for rapid electrochemical and colorimetric detection of influenza virus. Reprinted with permission from [60], 2019 Elsevier. C) A capillary-flow immunoassay for detecting anti-SARS-CoV-2 nucleocapsid protein antibodies. Reprinted with permission from [61], 2021 ACS Publications. D) A paper-based antigen sensing platform using plant-derived monoclonal antibodies for detecting SARS-CoV-2. Reprinted with permission from [69], 2023 Elsevier.

few μL on the paper surface) or by the mean of covalent bonding when several steps are required.

Based on physical adsorption, Ruan et al. immobilized capture antibodies to atrazine and acetochlor on a glass fiber conjugate pad by drop-casting method within a competitive LFA coupled to a 3D electrochemical analyzer [59]. The detection principle is based on the competition between analytes (atrazine/acetochlor) present in the sample and haptens (atrazine-BSA/acetochlor-BSA) dropped on an NC membrane (test lines) for the capture antibody sites, as shown in Fig. 2A. The capture antibodies were labeled with palladium/platinum nanoparticles (Ab-Pd@Pt NPs) that act as an artificial peroxidase for the electrochemical oxidation of thionine (THI) acetate in the presence of hydrogen peroxide, as determined by differential pulse voltammetry. Upon sample addition, analytes flow by capillary action to the test and control lines of the NC membrane, resulting in an electrochemical signal that is inversely proportional to the analyte concentration. Quantification of atrazine and acetochlor was achieved after cutting the test line sections and placing them in an electrochemical cell containing screen-printed electrodes located below the strips, resulting in detection limits equal to 0.24 ppb and 3.2 ppb for atrazine and acetochlor, respectively. The practical use of the developed LFA was investigated by analyzing well and river water samples, and an overall recovery of 90.8 % to 117 % was obtained.

To further improve the performance of flow-based immunoassays, a vertical flow assay was conceived for influenza virus detection within a sandwich configuration [60]. This format consists of vertically stacking a sample pad, a conjugate pad, an NC membrane strip, and an absorbent pad on a polyester backing film that was perforated specifically to allow bioelements flow during the assay, as depicted in Fig. 2B. In this configuration, H1N1 influenza viruses were captured by a specific HRP-tagged anti-influenza A HA (HRP-Ab) antibody that was previously immobilized on the conjugate pad by drop-casting method. The formed immunocomplexes flowed towards the NC membrane, on which the CE and RE were stencil-printed, while gold was deposited on the WE by Electron Beam Evaporation to form a gold paper-based electrode. Quantification of H1N1 influenza viruses was achieved with an anti-influenza A HA antibody (Ab-E) immobilized on the WE via 11-mercaptoundecanoic acid (11-MUA), which formed a self-assembled thiol monolayer (SAM) on the electrode. The carboxylic groups of MUA were then activated using N-(3-dimethylaminopropyl)-N′-ethylcarbodiimide hydrochloride (EDC) and N-hydroxysuccinimide (NHS), allowing for the formation of a strong amide bond (CO-NH) between the carboxylic groups of 11-MUA and the amino terminals of the antibody (Ab-E). Thanks to the use of a different pore size sample pad (pore size: 0.45, 11 μm) and the fast vertical flow design, the binding efficiency of the analyte/HRP-Ab on the conjugate pad was improved and the constructed vertical lateral flow was applied for the analysis of both standard buffer solution and saliva samples, resulting in detection limits equal to 3.3 PFU/mL and 4.7 PFU/mL, respectively. In addition to the use of physical adsorption for the immobilization of antibodies on paper pads, this method can also be utilized for the immobilization of antigens that can serve as bioreceptors as well as for the preparation of immunological PADs for antibody detection. In this framework, Henry's group reported a capillary flow immunosensor for electrochemical quantification of SARS-CoV-2 IgG antibodies (anti-N antibodies) using SARS-CoV-2 nucleocapsid protein (N-protein) as a bioreceptor [61]. The immunosensor was composed of assembled layers of hydrophilic polyester-based channels combining a blood-filtration membrane, a bare filter pad, an NC membrane, and a paper-based waste pad placed at the end of NC membrane to create a passive pumping system that automated the steps, as illustrated in Fig. 2C. Drop-casting method was used to store both the anti-IgG HRP antibodies and the nucleocapsid protein (N-protein) on the bare pad and the NC membrane, respectively. Upon the addition of the blood sample and phosphate buffer solution, anti-N antibodies present in the blood flow to the NC membrane and bind the N protein, while HRP-anti-IgG antibodies, driven by passive flow, bind SARS-CoV-2 immunocomplexes formed on the NC membrane surface. The electrochemical quantification of anti-N antibodies was accomplished by placing stencil-printed carbon electrodes on top of the NC membrane so that the WE was in contact with the N protein strip. By introducing only 10 μL of the blood sample, this novel configuration detected SARS-CoV-2 IgG antibodies as low as 10 ng/mL in less than 20 min.

As discussed in previous sections, the immobilization of bio-recognition elements by physical adsorption represents an effective and practical approach. However, the washing cycles generally required in immunoassay protocols can lead to the desorption of biomolecules that have not been firmly bound to the surface. This problem can be solved using different strategies that allow antibodies/antigens to be covalently immobilized on the paper surface, regardless of the number of wash cycles. One of the most common approaches to achieving covalent bonding of the biorecognition element is the integration of nanomaterials in the preparation of PADs due to their high surface-to-volume ratio, mass production, ease of functionalization, easy handling, and high stability.

Noble metal nanoparticles, and in particular gold nanoparticles (AuNPs), are among the most sought-after nanomaterials used for anchoring antibodies to the paper surface due to their ease of chemical/electrochemical synthesis, biocompatibility, and low cost. As demonstrated by Boonkaew et al., an anti-C-reactive protein antibody (anti-CRP Ab) was successfully immobilized on filter paper-based screen-printed electrodes through the use of AuNPs for the label-free detection of CRP [62]. Here, the WE separately printed with graphene-containing carbon ink was subjected to electrochemical deposition of AuNPs prior to immobilizing the anti-CRP antibody. The covalent immobilization of the capture antibody was achieved using cysteine SAMs grafted onto the surface of the gold-modified WE, which was then incubated with a mixture of EDC/NHS capable of converting the carboxyl groups of the cysteine to amine-reactive sulfo-NHS esters, ready to form a covalent amide bond with the anti-CRP capture antibody. The absence and presence of CRP were monitored by electrochemical impedance spectroscopy. Under optimal conditions, an increase in charge transfer resistance at the WE surface was observed in the range of 0.05–100 μg/mL, with a detection limit equal to 15 ng/ mL. The origami immunosensor was also applied for the determination of CRP in certified human serum samples, with satisfactory recoveries (98.0 %–103.9 %). Although the developed immunosensor is easy to manufacture, inexpensive (no labeled biomolecules are involved), and requires only 5 μL of sample for analysis, the time required to incubate the system with the solutions to be analyzed is at least 50 min, which somewhat hinders the on-site use of the developed immunosensor.

The same scheme was adopted by Pavithra et al. for the label-free detection of carcinoembryonic antigen (CEA) by the immobilization of an anti-carcinoembryonic antibody (anti-CEA Ab) on filter paper, but this time using a home-made gold nanoparticles ink (AuNPs-ink) to print the WE [63]. The latter was modified with mercaptoamine functionalized receptor SAMs (R1) composed of 2-mercaptoethylamine/4-aminobenzaldehyde generating amine groups that can be used as anchors for antibody immobilization. To covalently immobilize anti-CEA Ab on the WE, the functionalized surface was immersed in glutaraldehyde solution (1 % v/v) followed by the addition of EDC/NHS coupling agent to covalently attach the capture antibody through its carboxylic terminal. Using differential pulse voltammetry, a detection limit equal to 0.33 ng/mL was achieved when CEA was analyzed in phosphate buffer-spiked solutions. The excellent sensitivity demonstrated by this device can be ascribed to the oriented immobilization of the antibodies, through their carboxyl groups, implying that the fragment antigen-binding region (Fab region) was fully exposed to the analyte.

On the other hand, Cai's group combined AuNPs with other nanomaterials in the form of amino-functional graphene (NH_2-G) and thionine (Thi) nanocomposites, or multi-walled carbon nanotubes (MWCNTs) and Thi nanocomposites for the covalent immobilization of

capturing antibodies aimed at the detection of CEA and 17β-estradiol as part of label-free paper-based immunosensors [64,65]. In both works, the filter paper-based screen-printed WE was modified with a few drops of (NH_2-G/Thi) or (MWCNTs/Thi) nanocomposites previously incubated with a solution of AuNPs to promote its pairing with the amino groups of NH_2-G and MWCNTs. The corresponding antibodies were dropped onto the modified WE and stored at 4 °C for a few hours to allow for the complete interaction between amino groups on the antibodies and gold surface. The use of the reported nanocomposites allowed for the detection of CEA and 17β-estradiol at the picomolar level, thus providing portable and highly sensitive platforms for point-of-care analysis.

Besides, metal oxide nanomaterials such as zinc oxide nanorods (ZNRs) known for their biocompatibility, thermal stability, and high isoelectric point (IEP = 9.5) that facilitate the immobilization of low IEP proteins through electrostatic interactions were also investigated for the immobilization of human chorionic gonadotropin antibody, prostate-specific antigen antibody, and carcinoembryonic antigen antibody on a filter paper-based WEs [66]. The fabrication process involves first modifying three separate WEs with reduced graphene oxide (rGO), to improve the conductivity of the paper electrodes, by in-situ reduction of graphene oxide on cellulose fibers in the presence of hydrazine monohydrate and ammonia solution. Then, ZNRs were in situ grown on the paper surface by a simple low-temperature hydrothermal method, providing multiple sites for the conjugation of capturing antibodies. Nanocomposites composed of rGO and silver nanoparticles (AgNPs) were used as catalytic labels to modify the detection antibodies. Once the immunological sandwiches were constructed on the WEs, the latter were folded in a timed order below the CE and RE, which were printed together on another pad of paper to perform amperometric measurements. The proposed multiplexed immunosensor exhibited a wide linear range of 0.002–120 mIU.mL^{-1} for HCG, 0.001–110 ng/ mL for PSA, and 0.001–100 ng/ mL for CE, with limits of detection at the picomolar range.

Carbonaceous nanomaterials, such as carbon nanotubes (CNTs), which are abundant, chemically stable, highly conductive, and bearing several functional groups (eg., -OH, -COOH, -NH_2) are another category of nanomaterials frequently used in the preparation of biosensing platforms, including PADs.

For example, a paper-based electrochemical immunosensor was developed to detect avian influenza virus antigens (H5N1, H7N9, H9N2) using paper-based flexible CNT electrodes [67]. The construction of these immunosensors relied on the screen-printing of three distinct WEs on filter paper using a paste made of CNTs and polydimethylsiloxane (PDMS) which confers great flexibility to the electrodes. Antibodies specific to the H5N1, H7N9, and H9N2 antigens were covalently immobilized on the three WEs through the carboxylic groups of CNTs that were previously activated using EDC/NHS chemistry. For influenza virus antigen detection, about 10 μL of each antigen sample was sufficient to form the antigen-antibody complexes within 20 to 30 min of incubation. The immune responses were then measured by differential pulse voltammetry and resulted in limits of detection of 0.95 pM, 1.69 pM, and 0.72 pM for H5N1, H7N9, and H9N2 antigens, respectively. Moreover, the in-house made paper-based screen-printed electrodes based on MWCNT-PDMS paste can help in avoiding the physical weakness of the usual paper pads used in the preparation of PADs, without affecting their flexibility.

To further improve the sensitivity of paper-based immunosensors, platinum nanoparticles (PtNPs) were deposited on carboxylated single-walled carbon nanotubes (SWCNTs) for the covalent immobilization of anti-hepatitis C virus antibodies (anti-HCV Ab) on filter paper-based electrodes [68]. The paper WE was screen-printed using a graphene ink and left to dry before being modified with 1 μL of PtSWCNTs suspension obtained by deposition-precipitation method. To covalently anchor the anti-HCV Ab to the filter paper surface, the carboxyl groups on PtSWCNTs were activated using EDC/NHS chemistry, followed by the addition of the antibodies. The presence of HCV antigen in the sample solution hindered the electrochemical oxidation of the ferri/ferrocyanide redox probe $[Fe(CN)_6]^{3-/4-}$ as measured by differential pulse voltammetry. The developed electrochemical immunosensor showed a linear response in the range of 0.05–1000 pg/ mL, and a limit of detection equal to 0.015 pg/ mL.

Based on the same principle of EDC/NHS activation chemistry, cellulose nanocrystals (CNCs) with multiple carboxylic groups were used to covalently immobilize anti-SARS-CoV-2 antibodies, expressed in *Nicotiana benthamiana* plant, against the receptor-binding domain (RBD) of the SARS-CoV-2 spike protein [69]. In this study, CNCs were selected to modify the paper pad because they possess the unique properties of a high aspect ratio, high surface area, high mechanical strength, and liquid crystalline nature. Moreover, CNCs are rich in functional groups (-OH and -COOH) and can be obtained by sustainable and low-cost process which definitely fits with the PADs concept. Therefore, the filter paper was screen-printed with a three-electrodes system, and then the WE made of graphene ink was modified with a few drops of the aqueous solution of CNC-COOH to graft carboxylic groups on the surface of the WE. The EDC/NHS mixture was then added onto the CNC-modified electrode to activate the -COOH groups and thus covalently attach the capture antibodies to the paper surface, as demonstrated in Fig. 2D. The quantification of RBD protein was performed by incubating the WE for 2 h with 5 μL of sample solution. In order to wash the unbound analyte, the absorbent pad was folded under the detection pad during the wash cycles. By performing differential pulse voltammetry, spike protein was detected in the RBD concentration range of 0.1 pg/mL-500 ng/mL, with a detection limit of 2.0 fg/mL.

Silica nanoparticles (SNs) represent another family of nanomaterials that have been widely involved in the fabrication of biosensors. SNs are known for their high monodispersity, ease of synthesis, and rapid functionalization with silanol groups using various organosilane coupling agents such as (3-aminopropyl)triethoxysilane (APTES) and (3-mercaptopropyl)trimethoxysilane (MPTES), capable of forming covalent bonds with carboxyl and thiol groups, respectively.

Therefore, SNs were recently incorporated into a microzone-based paper immunosensor for monitoring the emerging pollutant ethinylestradiol (EE2) in water samples [70]. In this design, the filter paper was first patterned with wax to create a hydrophilic sensing microzone (7 mm in diameter) that was subsequently treated with plasma to introduce aldehyde groups on the exposed surface. After oxidizing the microzone, 3-aminopropyl functionalized SNs were added to form covalent silanol (Si-OH) bonds with the oxidized surface. The pendant amine groups on the amino-SNs were covalently conjugated to the capture antibody (anti-EE2 antibody) in the presence of glutaraldehyde. In this study, SNs conjugated to anti-EE2 antibodies were used as an immunocapture probe for the solid-phase extraction of EE2 from river water samples without any pre-treatment steps. Then, the paper microzone was transferred onto a screen-printed carbon electrode modified with electrochemically reduced graphene for the detection of the EE2 released from the immunocapture pad under acidic treatment. The proposed microzone-based PAD was able to detect as low as 0.1 ng/L of EE2 in standard solutions using square wave voltammetry. Moreover, five natural and spiked water samples were analyzed to validate the reliability of the proposed method, and the obtained recovery values ranged from 97.5 % to 103.7 %, indicating the high accuracy of the developed PAD.

3.3. Molecularly imprinted polymers (MIPs): artificial antibodies

Molecularly imprinted polymers (MIPs), also known as artificial antibodies, are synthetic materials that possess selective recognition sites that can bind a specific molecule (template) among others [71]. The first preparation of MIP on paper support was reported in 2013 when Ge et al. fabricated a microfluidic origami electroanalytical device based on MIP by its electropolymerization on a porous paper working

electrode [72]. This pioneering device comprises a central pad with CE and RE, surrounded by four foldable pads, each consisting of a sampling zone with an individual WE made of carbon, as depicted in Fig. 3A. Wax printing and screen-printing strategies were used to prepare the hydrophilic zones and the three electrodes on A4 paper, respectively. To enhance the conductivity of the proposed 3D origami sensor, a layer of AuNPs was grown on the paper surface via an in-situ mechanism. Grafting of the MIP as an artificial recognition element onto the paper support was achieved by a simple and fast electropolymerization of the monomer (*o*-phenylenediamine) in the presence of the template/target (D-glutamic acid). Finally, the analytical performance of this MIP-PAD was assessed by detecting D-glutamic acid in buffered solutions, using DPV, leading to a low LOD of 0.2 nM in a linear range of 1.2 nM–125.0 nM.

MIPs can also be incorporated into the paper supports in the absence of an applied potential, for example by in-situ formation of a boronic affinity-based MIP around the template immobilized on the surface of the paper electrode [73]. In such a design, the filter paper working electrode was modified with gold nanorods grown in situ to enable covalent capture of 4-mercaptophenylboronic acid (MPBA) via Au—S bonds. MIP cavities formation involved incubating the MPBA-modified paper electrode with an OVA solution (template) for 3 h, followed by the addition of a pre-polymerization mixture containing tetramethyl orthosilicate (TMOS) and phenyltriethoxysilane (PTEOS) for around 12 h. *Re*-binding of OVA to MPBA-MIP paper was monitored by DPV in the presence of SiO_2@Au nanocomposites labeled MPBA and cerium dioxide-modified nicked DNA double-strand polymers used as a signal tag. The steps required for the preparation of this MIP-based sandwich are described in Fig. 3B. Interestingly, boronate affinity was introduced in order to generate a double recognition of OVA, thus improving the selectivity of the proposed MIP. Although the preparation of this affinity MIP-based PAD took considerably more time than the electropolymerization process, a wide linear range from 1 pg/mL to 1000 ng/mL was obtained with a relatively low detection limit of 0.87 pg/mL for the OVA glycoprotein.

Another strategy that has proved successful and simple in anchoring MIP on the paper support involves drop-casting a pre-synthesized MIP onto the cellulose network of filter paper [74]. In this work, a nano-sized MIP built on Fe_3O_4@Au nanoparticles encapsulated with silica was constructed via a sol-gel method in the presence of serotonin, phenyltrimethoxysilane (PTMOS), and TMOS. As for the 3D electrochemical PAD, it was designed by first defining a hydrophilic working zone on filter paper using alkyl ketene dimer (AKD)-inkjet printing, coupled with screen-printing of electrodes on the paper surface. The detection zone was connected to a foldable sampling pad, enabling the analysis to be carried out, as demonstrated in Fig. 3C. At the end, the synthesized MIP was drop-cast on the WE, and 20 μL of the sample was added to the sampling pad. According to the results obtained with linear sweep voltammetry (LSV), 0.002 μM of serotonin was detected in buffered solutions within the analytical range of 0.01–1000 μM.

The high chemical stability of MIPs, in contrast to natural antibodies, allows for the easy loading of this (bio)receptor onto the paper electrode by mixing a prepared MIP with graphene ink and screen-printing it onto the paper surface. This strategy was reported by Amatatongchai et al. for the determination of patulin in food samples using a 3D origami electrochemical PAD [75]. In detail, patulin MIP was synthesized using 2-oxindole as the template, methacrylic acid (MAA) as a monomer, N,N′-(1,2-dihydroxyethylene) bis (acrylamide) (DHEBA) as cross-linker and

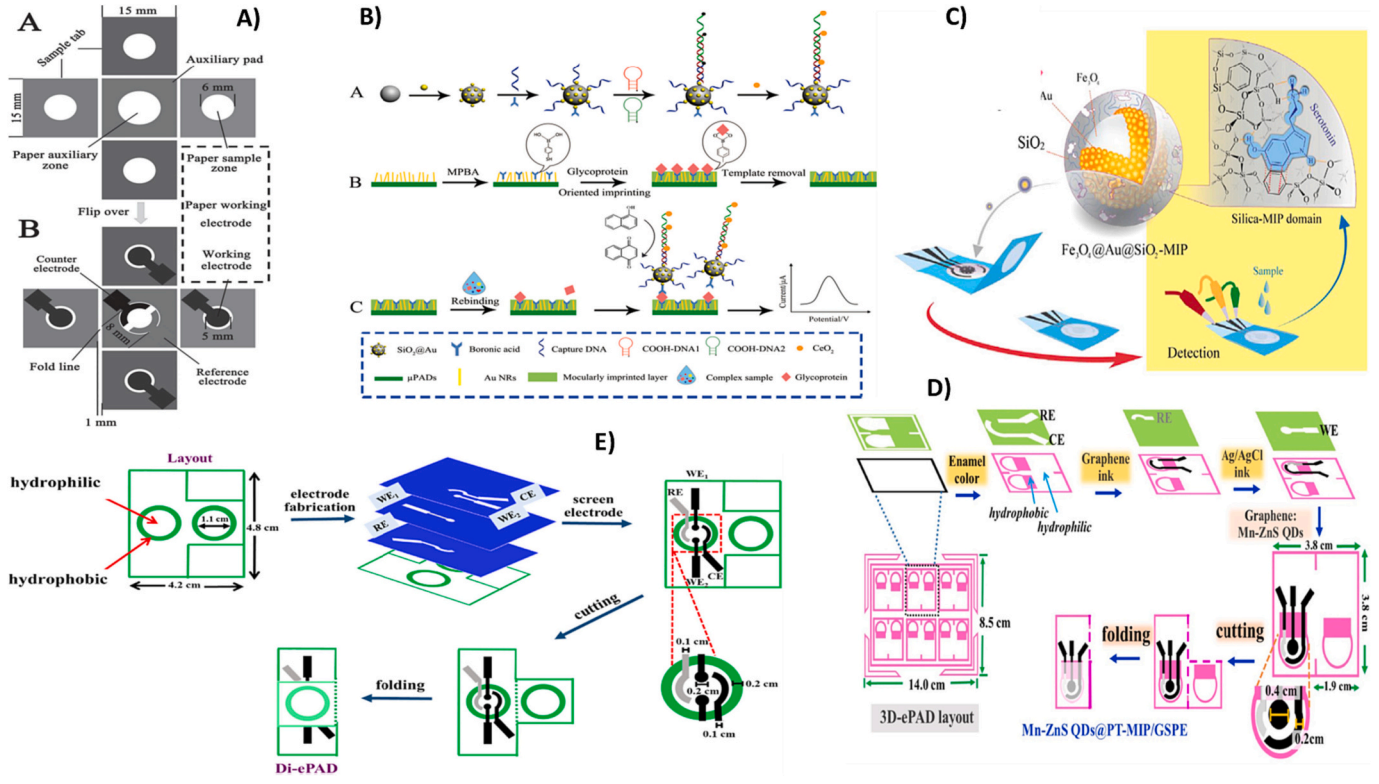

Fig. 3. A) Microfluidic electro-analytical origami device based on electropolymerized MIP for the of detection D-glutamic acid. Reprinted with permission from [72], 2013 Wiley Online Library. B) Microfluidic paper-based electrochemical biosensor based on a MIP film and boronate affinity sandwich assay for glycoprotein detection. Reprinted with permission from [73], 2019 ACS Publications. C). An electrochemical paper-based device composed of a graphite screen-printed electrode modified with a MIP coated with Fe3O4@Au@SiO2 for serotonin determination. Reprinted with permission from [74], 2019 Elsevier. D) Patulin-imprinted origami 3D-ePAD based on graphene screen-printed electrode modified with Mn–ZnS quantum dot coated with a MIP. Reprinted with permission from [75], 2023 Elsevier. E) Smart sensor for assessment of oxidative/nitrative stress biomarkers using a dual-imprinted electrochemical paper-based analytical device. Reprinted with permission from [76], 2022 Elsevier.

2,2′-azobis (2-methylpropionitrile) (AIBN) as initiator. Later, the as-prepared MIP was added to graphene ink to print the WE with patulin MIP. In this study, Whatman filter paper (Grade 1) was used as a support, while Penguard enamel color was employed to define hydrophobic barriers on the paper surface. Fig. 3D shows the fabrication of the ready-to-use imprinted PAD for patulin determination. Under the optimized conditions, the developed PAD revealed an excellent linear dynamic range of 0.001–25 μM, with a detection limit of 0.2 nM for patulin mycotoxin.

To offer a more advantageous MIP-based PAD enabling the simultaneous analysis of different biological matrices (e.g., urine, serum, whole blood), an alternative approach dealing with the imprinting of more than one template can be pursued. For instance, Amatatongchai et al. reported the development of a dual-imprinted electrochemical PAD to simultaneously determine 8-hydroxy-20-deoxyguanosine (8-OHdG) and 3-nitrotyrosine (3-NT) in urine and plasma samples [76]. To prepare this 3D origami device, the filter paper was screen-printed using a Penguard enamel color to define the hydrophobic borders surrounding two foldable working areas (sampling zone and detection zone), as shown in Fig. 3E. After constructing the circular hydrophilic zones, four electrodes (2 WE, 1 CE, 1RE) were screen-printed onto the detection zone to enable electrochemical sensing. To perform multiplexed detection of 8-OHdG and 3-NT, each WE was printed with graphene ink previously mixed with MIPs of 8-OHdG or 3-NT synthesized by successive self-assembly of L-cysteine on silica nanospheres decorated with silver nanoparticles. The dual-imprinted PAD revealed excellent linear dynamic ranges of 0.01–500 μM for 3-NT and 0.05–500 μM for 8-OHdG, with detection limits of 0.0027 μM and 0.0138 μM for 3-NT and 8-OHdG, respectively. Later, the same group succeeded in printing two different templates on the same MIP to ensure one-step detection of both 3-nitrotyrosine (3-NT) and 4-nitroquinolin-N-oxide (4-NQO) biomarkers [77]. In this case, the dual-MIP was prepared on GQDs-AuNPs via a (3-mercaptopropyl) trimethoxysilane (MPTMS) linkage and copolymerization with the 3-aminopropyltriethoxysilane (APTES) functional monomer, in the presence of both templates. To prepare the electrochemical sensor, the prepared dual-MIP was mixed with graphene ink before printing the WE on filter paper via a screen-printing approach. The developed dual-MIP revealed excellent linear dynamic ranges for both biomarkers of 0.01 to 500 μM for 3-NT and 0.005 to 250 μM for 4-NQO, with LOD equal to 0.002 μM and 0.001 μM for 3-NT for 4-NQO, respectively.

3.4. Nucleic acids

Nucleic acids (natural or synthetic) represent another type of bio-recognition element that has recently begun to be used in the manufacture of PADs.

In a simple configuration, a DNA genosensor was constructed on filter paper for the electrochemical detection of H1047R (A3140G), a single-stranded DNA (ssDNA) relative to a missense mutation in breast cancer [78]. The PAD was fabricated on filter paper-based screen-printed electrodes, using AuNPs to anchor recognition probes bearing a thiol group (-SH) at the 5′-terminus. In detail, the WE printed with graphite ink was modified with a few drops of an aqueous dispersion of gold nanoparticles to covalently immobilize the DNA probe sequences via the strong bonding between -SH groups and Au. The immobilization of the DNA probe was accomplished by incubating the WE with a 20 μL drop of probe for 60 min. Complementary hybridization between the probe and its target was monitored by performing signal ON and signal OFF approaches. The signal ON strategy relies on the addition of a positively charged redox mediator, ruthenium hexamine chloride ($Ru(NH_3)_6Cl_3$), which attaches to the negative backbone DNA double-stranded (dsDNA), while the signal OFF strategy was achieved by immobilizing a DNA probe labeled with methylene blue (MB) whose oxidation signal decreases upon formation of the duplex structure (dsDNA), thus hindering electron transfer between the MB and the electrode. Both approaches showed a wide linear range in the nanomolar window, and detection limits equal to 5 nM and 6 nM for the signal ON and signal OFF approaches, respectively.

To deliver a self-powered genosensor, Liu et al. developed an origami PAD with a pop-up structure for the electrochemical detection of adenosine 5-triphosphate (ATP) assisted by GOx-triggered reaction [79]. The design of the PAD was inspired by pop-up greeting cards to allow the fluidic path to be changed from supercapacitor to electrochemical mode. The origami PAD was composed of different areas, including an electrode tab, a detection zone, a reaction zone, a hollow area, and a supercapacitor tab, patterned on Whatman filter paper (grade 2) using a wax printing method. Again, the detection zone and the reaction zone were spatially separated to ensure no fluid connection between them prior to analysis. The quantification of ATP was based on the formation of a sandwich structure between: i) a DNA probe (DNA1) modified with a thiol group and immobilized by an Au-SH bond on the detection zone previously modified with AuNPs grown in situ, ii) an aptamer sequence specific to ATP capture, and iii) a GOx-modified DNA sequence (DNA2-GOx) capable of hybridizing with the aptamer. The presence of ATP in the sample resulted in the cleavage of the aptamer-DNA2-GOx due to the specific capture of ATP by the aptamer, leading to the release of DNA2-GOx onto the detection zone. To operate the supercapacitor mode, the detection zone was overlapped with the reaction zone in a clockwise direction, resulting in the flow of GOx from the detection zone to the reaction zone upon the addition of a phosphate buffer. In the reaction zone, GOx can catalyze the oxidation of glucose, pre-loaded on the reaction zone, leading to the conversion of $K_3[Fe(CN)_6]$ to $K_4[Fe(CN)_6]$, generating a voltage that was used to charge the paper supercapacitor. After washing the detection zone, the latter was overlapped with the electrode tab in a counterclockwise direction to perform differential pulse voltammetry measurements, given that GOx-DNA2 that was still bound to the aptamer in the detection zone could catalyze the oxidation of glucose in the presence of ferrocenecarboxylic acid, used as an electron transfer mediator. Fig. 4A illustrates the assay procedure of the developed PAD with dual-mode transduction. The proposed self-powered origami PAD enabled sensitive diagnosis of ATP in a linear range of 10–5000 nM with detection limits of 3 nM and 1.4 nM, in the case of supercapacitor and electrochemical modes, respectively. Furthermore, the employment of the pop-up configuration enabled dual-mode detection of ATP by simply folding the device in the desired direction.

As reported by Lu et al., the immobilization of the DNA probe on the paper support can also be achieved by using a conductive nanocomposite to modify the WE [80]. In that work, a ssDNA probe was immobilized on a cellulose membrane by the mean of a nickel metal-organic framework (Ni-MOF) composite/AuNPs/CNTs/polyvinyl alcohol (PVA), referred to as Ni—Au composite/CNT/PVA. To immobilize the DNA probe, a flexible electrode was fabricated by modifying cellulose with a solution of PVA and CNT mixtures using the vacuum filtration method. The flexible electrode was then modified with a few drops of Ni—Au composite previously prepared by the solvothermal method, then the DNA probe was deposited by casting method. The as-prepared electrode was then employed for the quantification of target human immunodeficiency virus (HIV) DNA using methylene blue (MB) within a signal OFF approach as shown in Fig. 4B. The developed PAD demonstrated excellent analytical performance with a linear range of 10 nM-1 μM and a low detection limit of 0.13 nM. Actually, the introduction of the Ni—Au composite on the cellulose surface improved the loading capacity of the ssDNA probe, compared to the electrode modified only with PVA/CNT, which can be explained by the high specific surface of Ni—Au that offers several hydrogen bonds to interact with the probe.

Apart from natural nucleic acids, PNAs (or peptide nucleic acids) have recently emerged as an alternative to conventional DNA. PNAs are synthetic oligonucleotides, comprising a repeating unit of N-(2 aminoethyl)-glycine linked to a peptide, replacing the sugar-phosphate

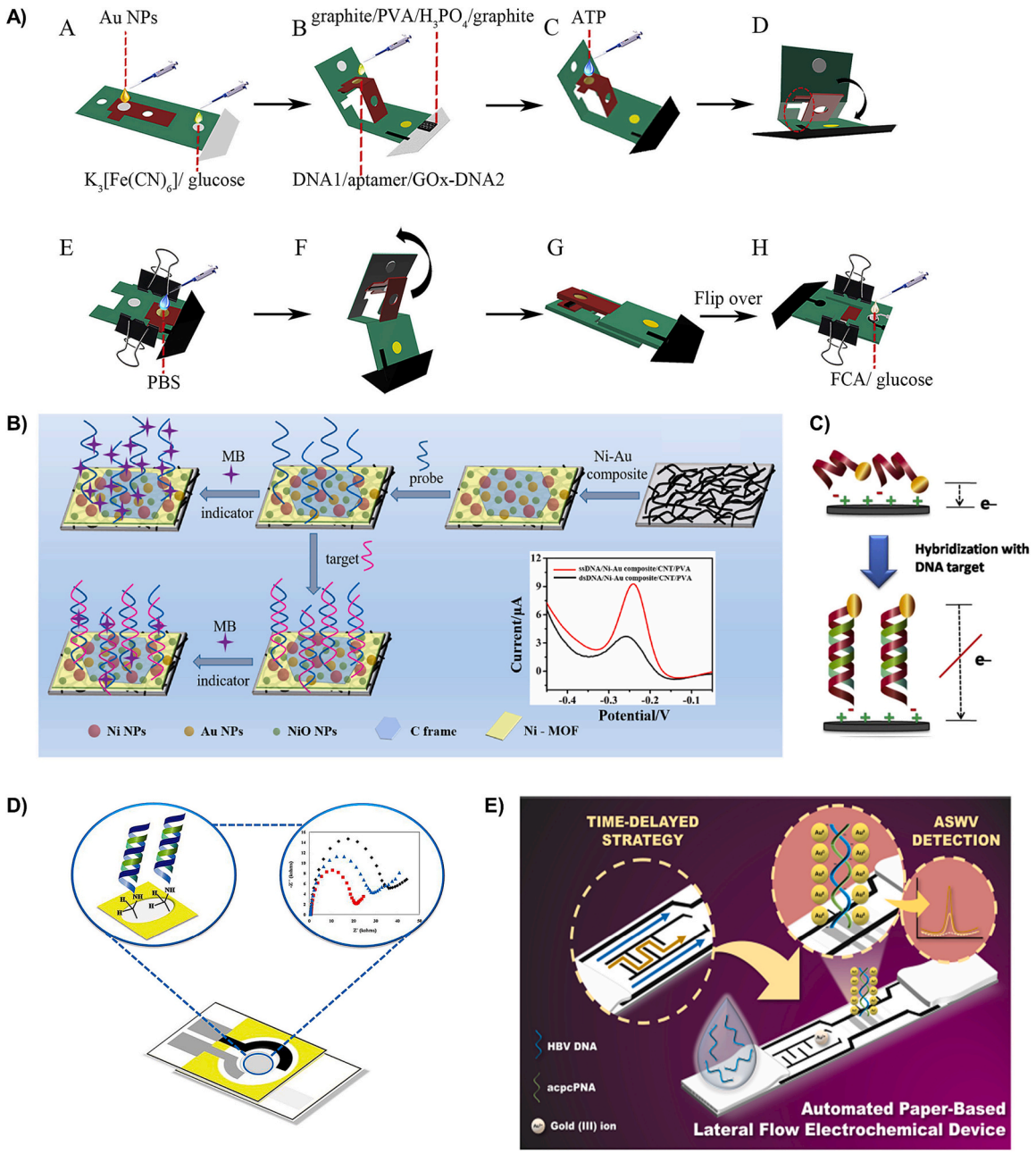

Fig. 4. A) A self-powered origami paper analytical device with a pop-up structure for dual-mode electrochemical sensing of ATP assisted by glucose oxidase-triggered reaction. Reprinted with permission from [79], 2020 Elsevier. B) A flexible paper-based electrode for HIV DNA detection. Reprinted with permission from [80], 2021 Elsevier. C) Electrochemical paper-based peptide nucleic acid biosensor for detecting human papillomavirus. Reprinted with permission from [83], 2017 Elsevier. D) An electrochemical impedance-based DNA sensor for tuberculosis detection. Reprinted with permission from [84], 2018 Elsevier. E) A paper-based lateral flow DNA device based on the amplification-free one-step detection of the Hepatitis B Virus. Reprinted with permission from [86], 2020 ACS Publications.

in natural DNA/RNA [81]. PNAs are uncharged; they have an electrostatically neutral structure that offers greater stability in nucleic acid hybridization. In addition, PNAs are resistant to nuclease and protease enzymes and bind strongly to target DNA. Among the PNA systems available, the pyrrolidinyl peptide nucleic acid (known as acpcPNA) invented by Vilaivan's group, has exceptional features that make it a powerful detection probe. AcpcPNA has an α,β-peptide backbone derived from D-proline/2-aminocyclopentanecarboxylic acid, which enables stronger affinity and higher sequence specificity for DNA and RNA binding, compared with the original aegPNA [82]. In addition, acpcPNA also offers the characteristic selectivity of antiparallel/parallel binding to the target and a low tendency to self-hybridization. Moreover, acpcPNA can be modified at the nucleobase or backbone level to incorporate various functionalities.

Within this framework, Teengam et al. reported the immobilization of acpcPNA on graphene-polyaniline (G-PANI) modified paper electrodes for the electrochemical detection of human papillomavirus (HPV) DNA [83]. Briefly, a three-electrode system was printed on filter paper by screening carbon ink as WE and CE, while Ag/AgCl was screened as RE. Then, six layers of G-PANI composite solution obtained by a physical mixing method were printed on the surface of the WE using an inkjet printing method. Prior to immobilization of the neutral acpcPNA probe, the latter was modified with three glutamic acid residues at the N-terminus to attribute a negative charge, while the C-terminus was conjugated to anthraquinone (AQ), an electroactive label. Immobilization of the AQ-PNA probe was achieved, by electrostatic interaction, by

depositing a 3 μL drop of the acpcPNA probe on the WE modified with the positively charged G-PANI composite. Detection of HPV DNA target was achieved by incubating the prepared WE with 3 μL of target DNA for 15 min. As a result of hybridization between acpcPNA and target DNA, the oxidation signal decreases significantly due to the increased rigidity of the PNA-DNA duplex compared to the native PNA probe, as illustrated in Fig. 4C. This rigidity impedes electron transfer between the redox-active (AQ) label and the electrode surface. Under the optimized conditions, the quantification of HPV DNA resulted in a linear response in the analytical range of 10–200 nM, with a detection limit of 2.3 nM, as measured by square wave voltammetry.

The acpcPNA probe was also used as a synthetic bioreceptor for the specific detection of *Mycobacterium tuberculosis* (MTB) using a filter paper-based origami biosensor [84]. The PAD developed consists of two layers: layer A holding the CE and RE printed with graphene-carbon ink and Ag/AgCl, respectively, and layer B bearing the WE made with carbon-graphene ink, as presented in Fig. 4D. The immobilization procedure of the acpcPNA probe on the backside of the WE involved the formation of covalent bonds on the partially oxidized surface of the electrode, according to the principle of periodate oxidation. By overlapping the two layers, the formation of a DNA-PNA duplex results in an increase in charge transfer resistance (R_{ct}) of $[Fe(CN)_6]^{3-/-4}$ redox probe as measured by electrochemical impedance spectroscopy. The analysis of increasing MTB concentrations was carried out by injecting the sample on layer A, resulting in a linear calibration curve in the 2–200 nM range with a detection limit of 1.24 nM. The PAD designed in the present study offers several advantages: it is very easy to manufacture, it does not require labeled sequences which generally increase manufacturing costs, and the immobilization strategy is suitable for all non-modified PNA probes.

The same PAD configuration was recently developed for the diagnosis of severe acute respiratory syndrome coronavirus 2 (SARS-CoV-2) using a specific acpcPNA probe immobilized on filter paper-based electrodes [85]. The immobilization of the acpcPNA probe was achieved by covalent bonding based on the periodate oxidation protocol. The only difference in PAD construction was to equip the WE layer with a loading channel to create a redox reporter loading channel. By folding the two layers on top of each other, a closed device was formed for the electrochemical determination of SARS-CoV-2 DNA by monitoring the behavior of $[Fe(CN)_6]^{3-/-4}$ redox probe using amperometric measurements. The proposed DNA sensor was successfully applied to the construction of a calibration curve in the range of 0.1 nM–200 nM, achieving a detection limit of 1 pM. The practical use of this device in the analysis of human serum samples was confirmed by the obtention of satisfactory recovery values in the range from 96.5 % to 104.5 %.

The same group later developed an automated paper-based LFA for the detection of hepatitis B virus (HBV) using a specific acpcPNA probe pre-loaded onto an NC membrane [86]. The LFA device was built using a printed-delayed configuration to enable automated reagent flow, as illustrated in Fig. 4E. The detection platform comprises four sections: i) a straight non-delayed channel serving as a sample pad, ii) a delayed zigzag channel pre-loaded with Au^{3+} ions, iii) a detection zone made of nitrocellulose and pre-loaded with an acpcPNA probe by the drop-casting method, and iv) an absorption pad responsible for the passive flow of reagents. For electrochemical detection of HBV DNA in the sample solution, a screen-printed electrode was placed under the NC membrane. Once the sample solution is added, HBV-DNA flows rapidly through the non-delayed channel and hybridizes with the acpcPNA probe pre-loaded on the detection zone. In contrast, the solution flowing through the zigzag channel is delayed by the wax barriers printed on it. Benefiting from this difference in flow velocity, PNA-DNA hybridization occurs first, followed by Au^{3+} binding to the captured DNA via electrostatic interactions. HBV-DNA analysis was performed by electrochemical reduction of captured Au^{3+} to form Au^0 metallized-DNA, followed by an anodic stripping voltammetry assay to determine HBV-DNA concentration via the gold signal. With this time-delayed microfluidic design, the total time required by the developed LFA to perform the entire assay was 7 min, with a wide dynamic range (10 pM to 2 μM) and a very low detection limit (7.23 pM). In addition, the use of an electrostatically neutral PNA probe minimized background current, as no interaction occurs between the PNA probe and Au^{3+} unless HBV DNA is present.

3.5. Aptamers

Aptamers are single-stranded oligonucleotides designed by a combinatorial selection process called Systemic Evolution of Ligands by Exponential Enrichment (SELEX) [87]. They are generally 100 base pairs in length and can be isolated from DNA or RNA libraries. Compared with antibodies, aptamers show lower immunogenicity, higher affinity, and excellent selectivity. One of the main advantages of aptamers is their ability to bind a wide range of targets, including those that are not immunogenic.

One of the very first approaches used to immobilize aptamer sequences on paper supports relied on the use of polystyrene microbeads functionalized with streptavidin as anchoring points [88]. The aptasensor PAD was printed on a single layer of paper with two different parts, folded into a 3D configuration. On one of the parts, an inlet area was created by wax printing, from which two identical channels were designed, as illustrated in Fig. 5A. At the end of their paths, the channels recombined to form two electrochemical half-cells. On the second side, two electrodes were screen-printed with conductive carbon ink. Once the paper was folded at the predefined fold line, the electrodes overlapped in the region where the channels recombined, forming the two electrochemical half-cells joined by a thin fluidic channel that acts as a salt bridge. This microfluidic structure was used to immobilize a capture aptamer specific to adenosine, whose presence induces cleavage of the GOx previously conjugated to the aptamer sequence. In detail, biotin-labeled aptamers specific to adenosine and conjugated with GOx were immobilized on 10 μm diameter polystyrene (PS) microbeads whose surface was functionalized with streptavidin. Next, a few drops of the prepared conjugates were added to one of the prepared channels, while no aptamer was loaded on the microbeads in the second channel, which was used as a control. When the sample is loaded at the inlet, the target flows through the microfluidic network and binds aptamer, inducing the release of GOx. The released enzyme then catalyzes the oxidation of glucose, resulting in the conversion of $[Fe(CN)_6]^{3-}$ to $[Fe(CN)_6]^{4-}$, generating a voltage that was used to charge a capacitor connected to the paper. In the present work, the immobilization of aptamer sequences using polyester microbeads eliminated the need for a washing step to remove excess probes, thus greatly facilitating the fabrication of this PAD. In addition, the microfluidic design presented here enables the sensor to operate as a self-powered unit, generating an output voltage without the need for an external power source. Also, by connecting the system to a digital multimeter, the accumulated capacitor is immediately discharged, enabling voltage readings to be taken in seconds. In the end, the origami system developed succeeded in detecting 11.8 μM of glucose when analyzing phosphate buffer-spiked solutions.

Later, Jiang et al. demonstrated that aptamer immobilization on an origami paper support can also be achieved by exploiting the negative charge of the aptamer backbone [89]. In this case, a paper microchannel array was designed on a chromatography paper by PDMS patterning, while the electrodes (WE, CE, and RE) were obtained by screen-printing conductive inks. Again, the WE was printed separately from the CE and RE to avoid contamination of the electrochemical cell during the functionalization procedure on the WE. The origami configuration consists of a sample loading pad comprising a central sample inlet with two hydrophilic channels carrying the CE and RE at their ends to form the detection zone. The latter is connected to a second pad holding the WE, which can be folded to complete the electrochemical system. The label-free detection of Ara h1, a food allergen, was achieved using a specific aptamer that was immobilized on the WE by electrostatic interaction.

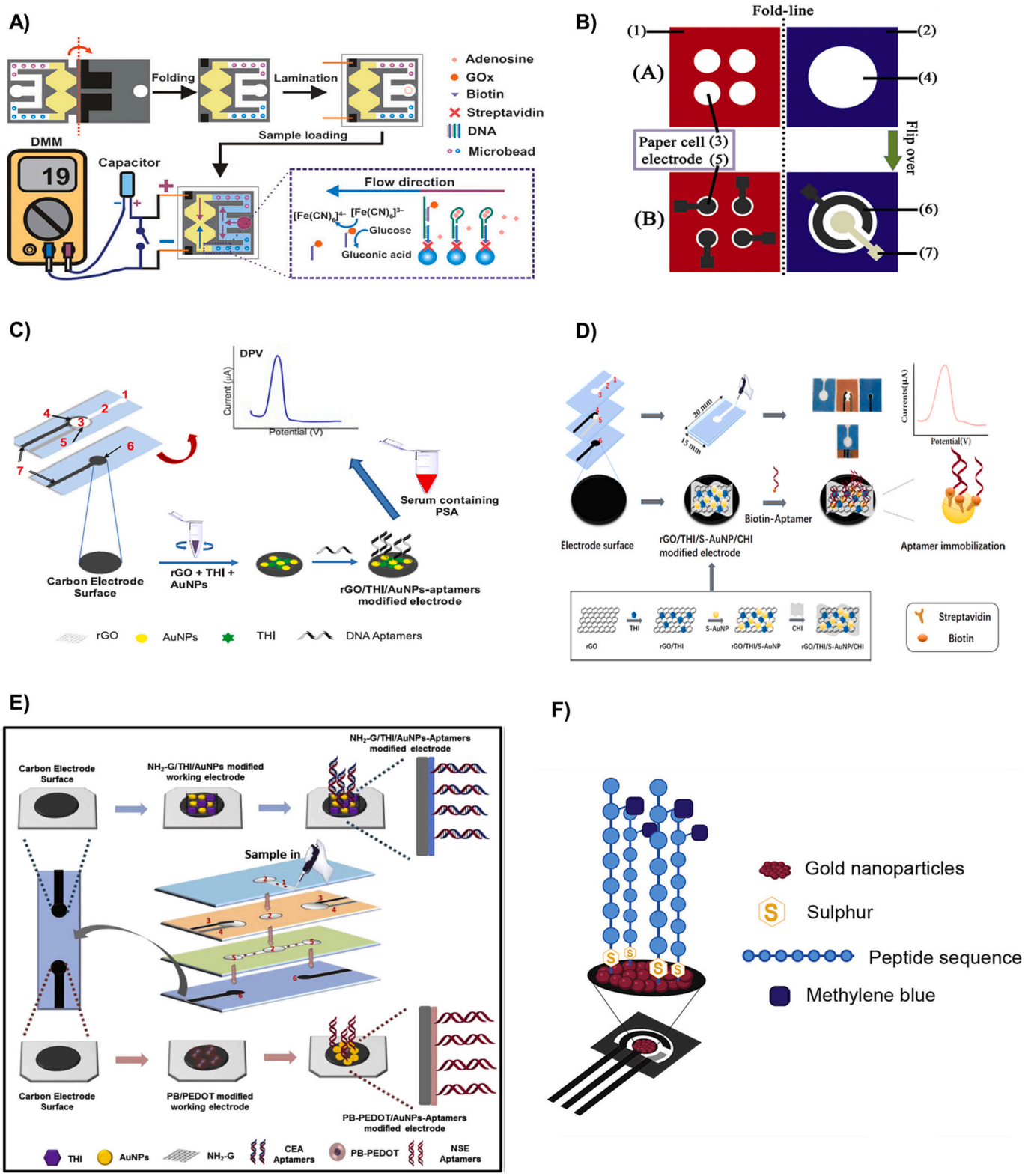

Fig. 5. A) Aptamer-based origami paper analytical device for electrochemical detection of adenosine. Reprinted with permission from [88], 2012 Wiley Online Library. B) A paper-based electrochemical cyto-device for sensitive detection of cancer cells and in situ anticancer drug screening. Reprinted with permission from [90], 2014 Elsevier. C) A paper-based electrochemical aptamer sensor modified with graphene nanocomposites for rapid and highly sensitive detection of prostate specific antigen. Reprinted with permission from [91], 2018 Elsevier. D) A microfluidic paper-based aptasensor based on a biotin–streptavidin system for label-free detection of biomarkers. Reprinted with permission from [93], 2021 ACS Publications. E) A label-free microfluidic paper-based aptasensor for ultrasensitive and simultaneous multiplexed detection of cancer biomarkers. Reprinted with permission from [94], 2019 Elsevier. F) A paper-based peptide sensor for on-site detection of botulinum neurotoxin serotype A and C. Reprinted with permission from [96], 2021 Elsevier.

First of all, the WE was modified with a 5 μL drop of black phosphorus nanosheets previously incubated with a polylysine solution to turn their charge positive. Then, the immobilization of Ara h1 aptamer was achieved by incubating the functionalized WE with 5 μL of the negatively charged aptamer. In a total time of 20 min, the proposed platform showed a good linear response in the range of 50–1000 ng/mL with a detection limit of 21.6 ng/mL, as monitored by differential pulse voltammetry. Thanks to the PAD design, a dual detection of the peanut allergen Ara h1 was achieved on a single origami microfluidic chip offering a more accurate analysis.

Being biocompatible, gold nanoparticles are among the most extensively studied nanomaterials for immobilizing aptamers on paper. For instance, an aptamer-based 3D macro-porous gold paper electrode was fabricated and used for the specific capture of human acute promyelocytic leukemia cells (HL-60) [90]. The origami PAD was constructed on Whatman chromatography paper (grade 114) and composed of a paper cell pad (red square) and an auxiliary paper pad (blue square) of identical dimensions, as depicted in Fig. 5B. On the paper cell tab, four circular hydrophilic zones were delineated with wax and then screen-printed with carbon ink to form four working electrodes. Regarding the auxiliary paper pad, it was shaped to contain a circular paper macro-zone, then printed with one CE and one RE designed to cover the four working electrodes printed on the paper cell pad. Before immobilizing the HL-60 cell-specific KH1C12 aptamer, each WE was modified with in-situ grown AuNPs, and then a 10 μL drop of KH1C12 aptamer was added. The modification of the cellulose surface with AuNPs not only improved the electrical conductivity of the paper cell zone but also considerably enlarged the adsorption surface of the aptamer. Specific capture of HL-60 cells by the immobilized aptamer was controlled by the addition of horseradish peroxidase-labeled folic acid (HRP-FA). The HRP-FA bioprobe enables both specific recognition of the folate receptor expressed on the surface of captured HL-60 cells and amplification of the electrochemical signal based on HRP-catalyzed *o*-phenylenediamine oxidation in the presence of H_2O_2. By requiring only 10 μL of HL-60 cell suspension, a wide linear range was obtained, from 5.0 10^2 to 7.5 10^7 cell mL^{-1}, as well as a detection limit equal to 350 cells mL^{-1}. Interestingly, the use of biocompatible AuNPs to prepare this cyto-origami device preserved the activity of captured live cells (HL-60 cells), which were used for in-situ screening of anticancer drugs by monitoring the apoptosis of these cells.

The immobilization capacity of AuNPs was also studied in combination with other nanomaterials, each playing a specific role in the preparation of aptamer-based PADs. As reported by Wei et al., the use of a nanocomposite consisting of AuNPs, rGO, and THi not only covalently anchored the aptamers to the cellulose network but also enhanced electron transfer on the paper surface [91]. In this work, the paper microfluidic device was built on pure cellulose paper by defining the hydrophilic pathways using a wax printing method, followed by screen-printing the WE, CE, and RE on two different paper layers, as shown in Fig. 5C. In fact, the first paper layer was designed to contain a sample inlet connected to a microchannel capable of transporting the analyte until the CE and RE areas, which were printed on the same cellulose layer. The second paper layer is dedicated to the WE, designed just below the CE/RE zone to collect the sample penetrating through the paper in a vertical flow. The immobilization of the aptamer specific for prostate-specific antigen (PSA) on the WE was achieved by the addition of a 10 μL drop of AuNPs/rGO/THI nanocomposite previously obtained by a physical mixing method, followed by the casting of a 10 μL drop of aptamer solution. In this case, the aptamer probe was covalently immobilized on the WE surface by the formation of Au—S bonds between the AuNPs and the aptamer modified with a mercapto group. The specific capture of PSA by the immobilized aptamer resulted in a decrease in the oxidation peak of THi used as an electrochemical mediator. In the end, the electrochemical aptamer sensor developed was able to detect PSA concentrations as low as 10 pg/ mL in serum samples, with a dynamic range from 0.05 to 200 ng/ mL. As demonstrated in this work, combining AuNPs with other nanomaterials could increase the aptamer immobilization surface, enhance electron transfer on the paper surface, and trap the electrochemical mediator.

The same 2-layer PAD configuration was later designed for the determination of programmed death ligand 1 (PD-L1) by means of a specific aptamer covalently immobilized on filter paper using AuNP nanocomposites [92]. In this work, a nanocomposite comprising amine-functionalized single-walled carbon nanotube (NH_2-SWCNTs), methylene blue (MB), and gold nanoparticles (AuNPs) was prepared and used to modify the WE. The use of amine-functionalized SWCNTs not only improved the electronic conductivity of the WE, it also promoted the anchoring of a greater number of AuNPs via Au-NH_2 interactions, thus covalently immobilizing a greater number of aptamers modified with sulfhydryl (-SH) groups. Utilizing MB as an electrochemical mediator adsorbed on the WE, the developed aptasensor showed a wide linear range between 10 pg/ mL and 2.5 ng/ mL, with a detection limit of 10 pg/ mL when analyzing phosphate-buffered saline solutions spiked with increasing concentrations of PD-L1.

The same group evaluated the synergistic effect between AuNP-based nanocomposites and the affinity-binding interaction between biotin- and streptavidin-labeled molecules for the immobilization of large quantities of aptamers on cellulose paper [93]. As can be seen in Fig. 5D, the paper sensor used in this work consists of three overlapped layers of paper; one carries a sample inlet connected to a microchannel, the second contains the CE and RE, and the third layer is printed with a WE alone to avoid any possible contamination of the other layers. The WE was modified with a 10 μL drop of amino redox graphene/THi/streptavidin-modified gold nanoparticles/chitosan nanoparticles (rGO/THi/S-AuNP/CHI), synthesized to firmly immobilize, and through the biotin-streptavidin pair, the aptamer probe labeled with biotin on its 5′ end. In this case, a 10 μL drop of aptamer solution was sufficient to modify the WE, which was then incubated for 6 h at 4 °C to form the sensing PAD. The principle of detection was based on the decrease in the THi oxidation peak in the presence of 17β-Estradiol (17β-E2), chosen as the model biomarker. Experimental results demonstrated that the developed label-free aptasensor is capable of determining 17β-E2 over a wide linear range of concentrations from 10 pg/ mL to 100 ng/ mL, with a detection limit equal to 10 pg/ mL. It's worth mentioning that the biotin-streptavidin pair, known for its greater stability, could render the sensor more stable over time, as predicted by the authors. However, a long incubation time was required to form the conjugated pair. In addition, blood samples had to be processed in advance to obtain the serum, limiting the on-site application of the developed PAD.

In another work, the same authors integrated AuNPs into two different nanocomposites for the immobilization of two different aptamers in order to detect carcinoembryonic antigen (CEA) and neuron-specific enolase (NSE) in serum samples using a single multiplexed device [94]. The microfluidic aptasensor was built from four stacked pieces of cellulose filter paper, giving it a filtering function. The first layer consists of a sample pad equipped with an inlet zone and a microchannel to allow for sample flow until it reaches the filter hole. The second layer contains two separate counter and reference electrodes, while the third layer holds two detection zones located exactly below the CE and RE. The final layer is the one printed with conductive carbon ink to form two separate WEs, as depicted in Fig. 5E. AuNPs nanocomposites combined with an amino-functional graphene (NG)-THi nanocomposites or Prussian Blue-poly (3,4- ethylenedioxythiophene) (PEDOT) nanocomposites were used for the immobilization of CEA aptamer and NSE aptamer, respectively. NG-THI-AuNPs nanocomposites were synthesized according to a physical mixing method as reported in the previous work, while Prussian Blue -PEDOT-AuNPs nanocomposites were obtained by the oxidative polymerization of EDOT in the presence of Fe^{3+} ions, followed by the addition of AuNPs solution. Each WE was incubated with a 10 μL drop of a single nanocomposite, followed by the casting of 10 μL of one of the aptamers. As the aptamers were modified with thiol groups on their 5′ end, they were covalently

immobilized on the corresponding WE through Au—S bonds. The presence of CEA and NSE was detected by monitoring the electrochemical oxidation of THi and Prussian Blue, respectively, used as electrochemical mediators. Under optimal conditions, the multi-parameter aptasensor exhibited good linearity in ranges of 0.01–500 ng/ mL and 0.05–500 ng/ mL for CEA and NSE, respectively. The limits of detection were found to be equal to 2 pg/ mL and 10 pg/ mL for CEA and NSE, respectively.

3.6. Other bioreceptors

In order to prepare a paper-based cyto-device for the capture of K-562 myelogenous leukemia cells, a concanavalin A (ConA) glycoprotein was immobilized on a paper-based WE for affinity binding of K-562 cells in a sandwich configuration [95]. The detection of K-562 cells was achieved by sandwiching them between a hybrid nanomaterial modified with ConA and deposited on WE and a ConA labeled with dendritic palladium-silver nanoparticles (PdAg NPs) acting as an artificial peroxidase. The origami paper design consisted of two foldable layers containing the WE separately from the CE and RE, which were screen-printed on the second layer of paper. ConA immobilization was achieved by depositing 10 μL of ConA solution on the WE previously modified with 10 μL of a 3D nanocomposite composed of gold nanoparticles and graphene (3D-AuNPs/GN). The WE thus prepared was incubated with a few μL of 1-ethyl-3-methylimidazoliumtetra fluoroborate ([BMIM]BF_4) ionic liquid and then used to capture K-562 cells. Here, the use of a 3D nanocomposite structure provides a higher specific surface area, which could bind more ConA by physical adsorption. Furthermore, the use of an ionic liquid mainly enabled high conductivity and good stability of the prepared electrode. After the specific binding between ConA and the mannose moieties present on the surface of K-562 cells, phorbol 12-myristate-13-acetate (PMA) was added to induce endogenous H_2O_2 generation by K-562 cells, to be detected by DPV in the presence of THi. The developed origami cyto-device exhibited a linear range comprised between 1.10^3 and 5.10^6 cells mL^{-1}, with a limit of detection of 200 cells mL^{-1}.

For a different application, our group used a peptide probe as a recognition element for the preparation of an electrochemical PAD capable of detecting botulinum neurotoxins (BoNT) produced by the bacterium *Clostridium botulinum* [96]. A synthetic peptide (Cysteine-(Ahx-Lys-Thr-Arg-Ile-Asp-Glu-Ala-Asn-Gln-Arg-Ala-Thr-Lys)-Methylene blue) was designed to contain 14 amino acids bordered at one end by cysteine, and by methylene blue at the other. The detection of BoNTs (A and C) was based on the capability of these toxins to cleave sites between Gln and Arg for BoNT/A and between Arg and Ala for BoNT/C, resulting in the loss of MB label. The construction of this peptide sensor relied on the modification of a screen-printed paper-based WE with a few μL of AuNPs solution, followed by the addition of the peptide probe. In this case, the peptide was covalently immobilized on the paper electrode by the formation of Au—S bonds via its cysteine residues, as demonstrated in Fig. 5F. After incubating the peptide-modified WE with a toxin solution for four hours, the electrochemical oxidation of MB was monitored in a signal-off approach using square wave voltammetry. Finally, the pairing of the developed PAD with a smartphone-assisted potentiostat enabled the detection of BoNT/A and BoNT/C with linearity up to 1 nM and a detection limit equal to 10 pM in phosphate buffer solutions.

4. Discussions

As discussed so far, the use of paper material has become a leading strategy in the development of electrochemical biosensors, especially for its suitability and advantages regarding the immobilization of bioreceptors used in biosensing.

A detailed analysis of the literature reviewed is reported in Table 3 in which some general trends emerge, pointing out the most common approaches used to immobilize each type of biocomponent on a paper platform. First of all, it is clear that Whatman filter paper (grade 1) is the paper support most used. An interesting insight to explain this preference is given by the presence of abundant hydroxyl groups on this kind of paper [24], which can improve the interactions occurring in the cellulose matrix, especially in the case of biocomponent loading by physical adsorption. Moreover, the porosity of this kind of paper facilitates the homogeneous loading of the biocomponents: typically, an aqueous solution containing the biocomponent is drop-cast on the paper (typically between 2 and 10 μL) and adsorbed within hydrophobic barriers through capillary forces.

Besides porous papers, office paper appears to be more suitable as a support for the printing of the electrodes since the narrower mesh of its cellulose network does not allow for the fast adsorption of the biocomponent solution. However, office paper can be used for cross-linking or polymerizing molecules as immobilization strategies, even if this paper is not able to work as a reservoir of reagents and as an equipment-free microfluidics system, because it is not a porous support.

Regarding the anchoring of the biocomponent, this is mostly dependent on the chemical properties of the biocomponent. For instance, enzymes are preferentially loaded on the paper by just physical adsorption, exploiting the adsorptive properties of porous types of papers. By contrast, antibodies, nucleic acids, and aptamers are more commonly anchored by chemical bonding between the functional groups of the biorecognition elements and the paper-based electrode (e.g., Au—S or Si—O interactions), eventually via linking reagents (e.g., EDC/NHS, glutaraldehyde). These strategies are suitable for paper types with different porosity. Furthermore, MIPs can be synthesized on porous Whatman paper via polymerization processes.

Overall, all the various strategies explored for developing electrochemical PADs have proved successful analyses of different matrices (e.g., blood, urine, tears, water, juice) with excellent analytical performances. The sensitivity can be improved by using nanomaterials, which can be efficiently applied on different paper surfaces and ensure good electrochemical performances and highly efficient biorecognition mechanisms. Additionally, the designing of 3D configurations, as well as the use of the porosity of the paper for the preconcentration of the target analyte, are features that could be further improved to develop novel and sensitive multi analysis detection, harnessing the immobilization of multi bioreceptors in different layers.

5. Conclusions and challenges

The considerable expansion of PADs can be justified by the exceptional characteristics of the paper material, which can be used for the: i) pre-treatment of the sample to be analyzed, ii) immobilization of biorecognition elements capable of specifically recognizing the analyte under consideration, iii) in-situ synthesis of nanomaterials, iv) passive transport of analyte/reagents by capillary forces, thus delivering pump-free devices, v) storage of all chemicals required for analysis, thus obtaining reagent-free devices, and vi) printing of electronic components to obtain an all-in-one device.

PADs can be combined with electrochemical transduction, thus improving sensitivity compared with optical methods. The excellent sensitivity achieved by electrochemical PADs guarantees their use in a variety of fields, including clinical diagnostics, environmental monitoring, and food control. The most popular electrochemical PADs are capable of operating in voltammetric modes, enabling precise and high-throughput target detection. In addition, PADs can be coupled to smartphone-based devices using commercially available miniaturized potentiostats, enabling on-site detection in a matter of minutes, as well as with machine learning combined with paper-based arrays to deliver smart multi-modal analytical devices.

On the other hand, the great flexibility of the paper support has enabled electrochemical PADs to be developed in different configurations ranging from paper-based microzones to vertical/lateral flow design, or even 3D microfluidic configuration involving the stacking or

Table 3
Summary of the principal features of electrochemical paper-based devices divided based on the different immobilized bioreceptors.

Bioelement		Immobilization strategy	Type of paper	Nanomaterial	Device configuration	Analyte	Analytical features			Ref
							LOD	Linear range	Matrix	
Enzyme	GOx LOx Uricase	Physical adsorption	Whatman filter paper #1	–	Paper-based SPE	Glucose Lactate Uric acid	0.21 mM 0.36 mM 1.38 mM	Up to 100 mM Up to 50 mM Up to 5 mM	Serum	[16]
	GOx	Physical adsorption	Whatman filter paper #1	–	Paper-based PDE coupled with waxed-patterned folding paper pad	Glucose	0.05 mM	1–12 mM	Blood	[39]
	GOx	Physical adsorption	Whatman filter paper #1	–	SPE coupled with waxed-patterned folding paper pad	Glucose	–	Up to 24 mM	–	[40]
	GOx	Physical adsorption	Cordenons filter paper	PBNPs	Paper-based SPE	Glucose	–	Up to 30 mM	Blood	[41]
	GOx	Physical adsorption	Whatman filter paper #1	CB - PBNPs	Paper card inserted in PVC electrochemical cell	Glucose	0.05 mM	0.2–2 mM	Tears	[42]
	Alcohol oxidase	Cross-linking	Office paper	CB - PBNPs	Paper-based SPE	Ethanol	0.52 mM	Up to 10 mM	Beer	[44]
	BChE	Physical adsorption	Cordenons filter paper - nitrocellulose paper	CB - PBNPs	Paper-based SPE coupled with filter paper strip and NC membrane	Paraoxon	3 µg/L	Up to 25 µg/L	River and wastewater	[45]
	BChE	Physical adsorption	Office paper	CB - PBNPs	Paper-based SPE	Paraoxon	1.3 ng/mL	Up to 25 ng/mL	Soil	[46]
	BChE	Physical adsorption	Whatman filter paper #1	CB - PBNPs	Paper-based SPE coupled with multiple wax-patterned folding paper pads	Methyl parathion	0.06 nm	0.1–1.0 nM	–	[47]
	BChE AP Tyrosinase	Physical adsorption	Filter and office paper	CB - PBNPs	Paper-based SPE coupled with multiple wax-patterned folding paper pads	Paraoxon 2,4-D Atrazine	2 ppb 50 ppb 2 ppb	2–20 ppb 100–600 ppb 10–100 ppb	River water	[48]
	AP BChE HRP	Physical adsorption	Filter and office paper	CB - PBNPs	Paper-based SPE coupled with flower-like wax-patterned folding paper pads	2,4-D Glyphosate Paraoxon	30 ppb 10 ppb 2 ppb	50–200 ppb 0–150 ppb 2–20 ppb	Aerosolized pesticides	[49]
	ChOx	Physical adsorption	Filter paper	CB - PBNPs ink	Paper-based SPE coupled with wax-patterned folding paper pad	SM	1 mM 0.019 g·min/m^3	Up to 6 mM Up to 6 mM	Liquid phase SM Aerosolized SM	[50]
	3-HBDH	Physical adsorption	Whatman filter paper #1	–	Paper-based SPE included in wax-patterned 3D paper structure	BHB	0.3 mM	0.1–6.0 mM	Blood	[51]
	PheDH	Physical adsorption	Filter paper n° 903	rGO	SPE coupled with wax-patterned paper pad	Phenylalanine	0.2 µM	1–600 µM	Blood	[52]
	GOx LOx	Physical entrapment	Whatman filter paper #1	$Ti_3C_2T_x$ Mxenes CB	Paper-based SPE coupled with wax-patterned folding paper pads	Glucose Lactate	17.05 µM 3.73 µM	0.08–1.25 mM 0.3–20.3 mM	Sweat	[53]
	GOx	Physical entrapment	Whatman filter paper #1	CB	Multiple polyester SPE coupled with hexadecagonalwax-patterned paper pad	Glucose	30 µM	0.1 - 40 mM	Urine	[54]
	Creatininase	Cross-linking	Filter paper	GQDs	Double polyester SPE coupled with hexadecagonalwax-patterned paper pad	Uric acid Creatinine	8.4 nM 3.7 nM	0.010–3.0 µM	Urine	[56]
	GOx	Covalent bond	Filter paper	rGO-TEPA/PB	Paper SPE SPE	H_2O_2	25 µM	0.1–25 mM	Sweat	[57]
Antibody	Haptens (Atrazine-BSA/ acetochlor-BSA)	Electrostatic adsorption	LFIA membrane cards	Pd@Pt NPs	Bifurcated LFIA strips	Atrazine Acetochlor	0.24 ppb 3.2 ppb	0.1–500 ppb 1–1000 ppb	River water	[59]
	HRP-tagged anti-A HA	Physical adsorption	Whatman filter paper #1	–	NC membrane wax-patterned electrode coupled with glass fiber pads and filter paper waste pad	H1N1	4.7 PFU/mL	Up to 10^4 PFU/mL	Saliva	[60]
	SARS-CoV-2 (N-protein)	Physical adsorption	Whatman filter paper #1	–	SPE coupled with vertical stacked polyester microfluidic network	SARS-CoV-2 IgG Ab	10 ng/mL	Up to 100 ng/mL	Blood	[61]
	Anti-CRP Ab	Covalent bond	Whatman filter paper #1	AuNPs	Paper-based SPE coupled with wax-patterned paper pads	CRP	15 ng/mL	0.05–100 µg/mL	Serum	[62]
	Anti-CEA Ab	Covalent bond	Whatman filter paper #1	AuNPs ink	Paper-based SPE	CEA	0.33 ng/mL	1–100 ng/mL	–	[63]

(*continued on next page*)

Table 3 (*continued*)

Bioelement		Immobilization strategy	Type of paper	Nanomaterial	Device configuration	Analyte	Analytical features			Ref
							LOD	Linear range	Matrix	
	Anti-CEA Ab	Covalent bond	Whatman filter paper #1	NH_2-G/ Thi/ AuNPs	Paper-based SPE	CEA	10 pg/mL	50–500 ng/mL	Serum	[64]
	Anti-E2	Covalent bond	Whatman filter paper #1	MWCNTs/ THI/ AuNPs	Paper-based SPE	17 β-estradiol	10 pg/mL	0.01–100 ng/ mL	Blood	[65]
	$HCG\text{-}Ab_1$ $PSA\text{-}Ab_1$ $CEA\text{-}Ab_1$	Covalent bond	Whatman filter paper #1	rGO/AgNPs/ ZNRs	Paper-based SPE coupled with wax-patterned paper pads	HCG PSA CEA	0.0007 mIU/mL 0.35 pg/mL 0.33 pg/mL	0.002–120 mIU/mL 0.001–110 ng/ mL 0.001–100 ng/ mL	Serum	[66]
	H5N1 Ab H7N9 Ab H9N2 Ab	Covalent bond	Whatman filter paper #1	CNTs	Multiple paper-based SPE	H5N1 H7N9 H9N2	0.95 pM 1.69 pM 0.72 pM	10–100 ng/mL	Serum	[67]
	Anti-HCV Ab	Covalent bond	Whatman filter paper #1	PtNPs/SWCNTs	Paper-based SPE	HCV	0.015 pg/ mL	0.05–1000 pg/ mL	Serum	[68]
	Anti-SARS-CoV-2 Ab	Covalent bond	Whatman filter paper #1	CNCs	Paper-based SPE coupled with wax-patterned folding paper pads	RBD protein SARS-CoV-2	2 fg/mL	0.1–500 ng/mL	Saliva	[69]
	Anti-EE2 Ab	Covalent bond	Whatman filter paper #1	RG SNs	SPE coupled with wax-patterned paper pad	EE2	0.1 ng/L	0.5–120 ng/L	Water	[70]
MIPs MIPs	OPD	Electropolymerization	Office paper	AuNPs	Paper-based SPE coupled with wax patterned multiple folding paper pads	D-glutamic acid	0.2 nM	1.2–125.0 nM	Serum	[72]
	MPBA TMOS/ PTEOS	Chemical polymerization	Whatman filter paper #1	SiO_2@AuNRs	Paper-based SPE coupled with wax patterned multiple folding paper pads	OVA	0.87 pg/mL	1 pg/mL - 1000 ng/mL	–	[73]
	TMOS/PTEOS	Chemical polymerization	Whatman filter paper #1	Fe_3O_4@Au@ SiO_2	Paper-based SPE coupled with wax patterned folding paper pads	Serotonin	0.002 μM	0.01–1000 μM	–	[74]
	MAA DHEBA AIBN	Chemical polymerization	Whatman filter paper #1	Mn–ZnS QDs@PT	Paper-based SPE coupled with wax-patterned paper pad	Patulin	0.2 nM	0.001–25 μM	Food	[75]
	NIPAM DHEBA	Thermal polymerization	Whatman filter paper #1	SiO_2@AgNPs	Paper-based SPE coupled with wax patterned circular folding paper pad	3-NT 8-OhdG	0.0027 μM 0.0138 μM	0.01–500 μM 0.05–500 μM	Urine Plasma	[76]
	MPTMS APTMS	Chemical polymerization	Whatman filter paper #1	GQDs-AuNPs	Paper-based SPE coupled with wax-patterned paper pad	3-NT 4-NQO	0.002 μM 0.001 μM	0.01–500 μM 0.005–250 μM	–	[77]
Nucleic acids and peptides	ssDNA	Covalent bond	Whatman filter paper #1	AuNPs	Paper-based SPE	H1047R (A3140G)	5 nM (on) 6 nM (off)	0.1–3000 nM	Blood	[78]
	ssDNA	Covalent bond	Whatman filter paper #2	AuNPs	Paper-based SPE included in wax-patterned 3D paper structure	ATP	3 nM (SC) 1.4 nM (EC)	0.01–5 μM	–	[79]
	ssDNA	Covalent bond	Cellulose membrane	AuNPs/CNTs	Paper-based SPE	HIV	0.13 nM	10 nM-1 μM	Serum	[80]
	acpcPNA (HPV)	Electrostatic interaction	Whatman filter paper #1	G-PANI	Paper-based SPE	HPV DNA	2.3 nM	10–200 nM	PCR samples	[83]
	acpcPNA (MTB)	Covalent bond	Whatman filter paper #1	G-PANI	Paper-based SPE coupled with wax-patterned folding paper pad	MTB DNA	1.24 nM	2–200 nM	PCR samples	[84]
	acpcPNA (SARS-CoV-2)	Covalent bond	Cellulose membrane	–	Paper-based SPE coupled with wax-patterned folding paper pad	SARS-CoV-2 (N gene)	1.0 pM	0.1–200 nM	Nasopharyngeal swab	[85]
	acpcPNA (HBV)	Electrostatic interaction	Nictrocellulose membrane	AuNPs	Paper-based SPE	HBV DNA	7.23 pM	10–2 μM	Serum	[86]
Aptamers	Ara h1 aptamer	Covalent bond	Whatman filter paper #1	BPNSs	Paper-based SPE coupled with wax-patterned folding paper pad	Ara h1	21.6 ng/mL	0.05–1 μg/mL	Food	[89]
	KH1C12 aptamer	Physical adsorption	Whatman filter paper #1	AuNPs	Paper-based SPE coupled with wax patterned folding paper pad	HL-60	350 cells/ mL	$5.0\,10^2$–$7.5\,10^7$ cell/mL	Live cells	[90]
	Anti-PSA apatmer	Covalent bond	Whatman filter paper #1	AuNPs/rGO/THI	Paper-based SPE	PSA	10 pg/mL	0.05–200 ng/ mL	Serum	[91]
	PD-L1 aptamer	Covalent bond	Whatman filter paper #1	NH2-SWCNT/ NMB/AuNPs	Paper-based SPE coupled wax-patterned folding paper	PD-L1	10 pg/mL	10 pg/mL - 2.5 ng/mL	Serum	[92]

(*continued on next page*)

Table 3 (*continued*)

Bioelement		Immobilization strategy	Type of paper	Nanomaterial	Device configuration	Analyte	Analytical features			Ref
							LOD	Linear range	Matrix	
	17β-E2 aptamer	Covalent bond	Whatman filter paper #1	rGO/THI/S-AuNP/CHI	Paper-based SPE coupled wax-patterned folding paper	17β-E2	10 pg/mL	10 pg/mL - 100 ng/mL	Serum	[93]
	CEA, NSE aptamers	Covalent bond	Whatman filter paper #1	AuNPs	Paper-based SPE coupled wax-patterned folding paper	CEA NSE	2 pg/mL 10 pg/mL	0.01–500 ng/mL 0.05–500 ng/mL	Serum	[94]
Other	ConA	Covalent bond	Whatman filter paper #1	3D-Au NPs/GN/PdAg NPs	Paper-based SPE coupled wax-patterned folding paper	K-562	200 cells/mL	1.10^3–5.10^6 cells/mL	–	[95]
	Synthetic peptide	Covalent bond	Whatman filter paper #1	AuNPs	Paper-based SPE	BoNTs	10 pM	Up to 1 nM	Orange juice	[96]

GOx = Glucose Oxidase, LOx = Lactate Oxidase, PDE = Pencil drawn electrode, PBNPs = Prussian Blue Nanoparticles, CB – PBNPs = Carbon Black-Prussian Blue Nanoparticles, 2,4-D = 2,4-D dichlorophenoxy acetic acid, BChE = Butyrylcholinesterase, AP = Alkaline phosphatase, NC = Nitrocellusose, HRP = Horse Radish Peroxidase, ChOx = Choline Oxidase, SM = Sulfur mustard agent, 3-HBDH = 3-Hydrozybutyrate Dehydrogenase, BHB = Beta-hydroxybutyrate, PheDH = Phenylalanine Dehydrogenase, rGO = Reduced Graphene, GQDs = Graphene Quantum Dots, Pd@Pt NPs = Palladium/Platinum nanoparticles, AuNPs = Gold Nanoparticles, anti-CRP Ab = anti-C-reactive protein antibody, CRP = C-reactive protein, anti-CEA Ab = anti-carcinoembryonic antibody, CEA = carcinoembryonic antigen, NH_2-G = amino-functional graphene, Thi = Thionine, MWCNTs = Multi-Walled Carbon Nanotubes, H5N1, H7N9, H9N2 = avian influenza virus antigens, HCV = hepatitis C virus, RBD = receptor-binding domain, SNs = Silica nanoparticles, EE2 = ethinylestradiol, RG = reduced graphene, OPD = *o*-phenylenediamine, MPBA = 4-mercaptophenylboronic acid, OVA = glycoprotein ovalbumin, TMOS = tetramethyl orthosilicate, PTEOS = phenyltriethoxysilane, Mn–ZnS QDs = Manganese-zinc sulfide quantum dots, MAA = methacrylic acid, DHEBA = co-N, N-(1,2-dihydroxyethylene) bisacrylamide, AIBN = 2,2′-azobis (2-methylpropionitrile), 8-OhdG = 8-hydroxy-2′-deoxyguanosine, 3-NT = 3-nitrotyrosine, NIPAM = N-isopropylacrylamide, GQDs-AuNPs = Graphene quantum-dot capped gold nanoparticles, MPTMS = (3-mercaptopropyl) trimethoxysilane, APTMS = 3-aminopropyltriethoxysilane, ssDNA = single-stranded DNA, acpcPNA = pyrrolidinyl peptide nucleic acid, HPV = Human Papilloma Virus, MTB = *Mycobacterium tuberculosis*, HBV = hepatitis B virus, Ara h1 = Peanut allergen, BP = Black phosphorus, HL-60 = Human acute promyelocytic leukemia cells, PD-L1 = Programmed death-ligand 1, BoNTs = Botulinum neurotoxin.

folding of different paper layers, each designed for a particular task.

As described in the present review, the manufacture of electrochemical PADs capable of detecting multiple (bio)chemical analytes relies on a decisive step which is the engineering of the paper surface with different biorecognition elements including enzymes, antibodies, nucleic acids, aptamers, and cells. Physical adsorption of these elements via a drop-casting method is the approach frequently used to modify the paper network. Indeed, this method is very simple to carry out, however, biomolecules can be lost by a single wash, which explains the use of this approach particularly in the case of enzymatic PADs, where the analysis simply consists of adding the sample to be analyzed without any further wash cycle. For multi-step analysis, the (bio)receptors need to be covalently immobilized on the paper surface to prevent their loss during the assay. Three main approaches have been reported in this respect; the first involves modifying the paper surface with gold nanoparticles, allowing recognition elements bearing a sulfhydryl group to be immobilized via Au-SH covalent bonds. The second approach relies on modifying the paper surface with carbon nanomaterials containing a terminal carboxylic group capable of attaching the recognition element via its pendant amino groups in the presence of the EDC/NHS linker. Another useful approach is to oxidize cellulose hydroxyl groups with a periodate, generating pendant aldehyde groups capable of forming an imine with the amino group of the biorecognition element.

The selection of a specific approach among others to combine biorecognition elements with PADs is not a random choice. In fact, the type of paper substrate (e.g., Whatman chromatography paper or nitrocellulose membrane), characterized by specific parameters such as pore size, porosity, functional groups, chemical stability, and physical strength, dictates the appropriate immobilization strategy that should not only ensure a high immobilization rate but also preserve the stability and activity of and activity of the bioreceptors.

Despite the growing use of electrochemical PADs, a number of challenges still hampering their widespread application and need to be pointed out. One of the most frequent problems is the easy contamination of PADs by dust and humidity in the ambient air, hence the need to use suitable packaging to store the prepared PADs for as long as possible, e.g., storage at 4 °C can help preserve the biocomponents.

Another challenge is the lack of stability of the bioreceptors over time, which in turn hinders the mass production and long-term storage of PADs. To ensure that biorecognition elements remain stable and active during PAD preparation and storage, several preservation approaches can be used depending on the bioreceptor. For example, it is well known that immobilizing enzymes on a solid carrier is one of the most widely used strategies for enhancing operational stability. Furthermore, adding polyols and sugars to aqueous enzyme solutions enhances hydrophobic interactions between non-polar amino acid residues, enabling enzymes to resist chemical changes. Certain preservatives such as polyethylene glycols and synthetic polymers (e.g., polyvinyl alcohol and polyvinyl pyrrolidone) can also be used, as they have been found to have a stabilizing effect on enzymes. Another biocompatible strategy is to entrap enzymes in polysaccharides (e.g., chitosan, alginate), which help to increase enzyme stability against proteolysis. On the other hand, antibodies, also require stabilization for long-term storage. Various stabilizers such as sugars (e.g., sucrose and trehalose) or polyols (e.g., glycerol and sorbitol) are frequently added to antibody preparation to preserve their native structure and inhibit physical instability during long-term storage of PADs. Other reagents, such as bovine serum albumin and tween-20, can be added to antibody preparation buffers, helping to increase antibody stability. In addition, certain preserving reagents such as sodium azide (0.05 %) or thimerosal (0.1 %) can also be used to prepare antibody formulations, helping to inhibit bacterial growth which adversely affects antibody stability. As far as nucleic acids are concerned, the use of DNA probes containing more G (and C) bases than A (and T) bases can contribute to the stability of double-stranded DNA over time. Similarly, the use of a working medium rich in monovalent alkali metal ions also stabilizes nucleic acid by

forming electrostatic interactions with the negative phosphate group of DNA. On the other hand, a higher salt concentration in the working buffer enhances base stacking interactions and thus the stability of the DNA duplex, as a high salt concentration prevents repulsion between two negatively charged DNA backbones.

The other issue still facing the emergence of electrochemical PADs is the relatively low sensitivity achieved compared to conventional electrochemical devices. Here again, many tactics have been employed by researchers to improve the analytical performance of electrochemical PADs, such as the use of conductive polymers or the incorporation of nanomaterials (e.g., carbon nanotubes, carbon black, graphene derivatives, MXenes, metal-organic frameworks) which not only help in improving the immobilization rate of bioreceptors on the paper surface but also guarantee good electron transfer.

In this overall scenario, the paper has paved the way for smart electrochemical devices able to i) work in complex matrices harnessing the electrochemical transduction and the porosity of the paper to treat the samples, ii) manage the sample and the reagents by capillary forces delivering equipment-free devices, iii) detect easily the target analytes in liquid and aerosol phase, and iv) easily immobilize the bioreceptors in a variety of configurations depending on the needs of the analytical tools selected in function of the target analyte, the concentration, and sample matrix, demonstrating that paper is a material that offers a plethora of features, working as a kaleidoscope in the electrochemical sensing field [97].

Declaration of competing interest

The authors declare that they have no known competing financial interests or personal relationships that could have appeared to influence the work reported in this paper.

Acknowledgments

F.A. and N.S. would like to thank Project E-Crome, A0375-2020-3656, Lazio Innova, Regione Lazio.

References

[1] World Commission on Environment and Development (Ed.), Our Common Future, Oxford University Press, Oxford; New York, 1987. W.
[2] Rosa (Ed.), A New Era in Global Health: Nursing and the United Nations 2030 Agenda for Sustainable Development, Springer Publishing Company, New York, 2017.
[3] P.T. Anastas, J.C. Warner. Green Chemistry: Theory and Practice, Oxford University Press, 1998.
[4] Galuszka, Z. Migaszewski, J. Namiesnik, The 12 principles of green analytical chemistry and the SIGNIFICANCE mnemonic of green analytical practices, TrAC Trends Anal. Chem. 50 (2013) 78–84, https://doi.org/10.1016/j.trac.2013.04.010.
[5] M. Nowak, R. Wietecha-Posłuszny, J. Pawliszyn, White Analytical Chemistry: An approach to reconcile the principles of Green Analytical Chemistry and functionality, TrAC Trends Anal. Chem. 138 (2021), 116223, https://doi.org/10.1016/j.trac.2021.116223.
[6] S. Cinti, D. Moscone, F. Arduini, Preparation of paper-based devices for reagentless electrochemical (bio)sensor strips, Nat. Protoc. 14 (2019) 2437–2451, https://doi.org/10.1038/s41596-019-0186-y.
[7] F. Arduini, Electrochemical paper-based devices: when the simple replacement of the support to print ecodesigned electrodes radically improves the features of the electrochemical devices, Curr. Opin. Electrochem. 35 (2022), 101090, https://doi.org/10.1016/j.coelec.2022.101090.
[8] E. Noviana, C.P. McCord, K.M. Clark, I. Jang, C.S. Henry, Electrochemical paper-based devices: sensing approaches and progress toward practical applications, Lab Chip 20 (2020) 9–34, https://doi.org/10.1039/C9LC00903E.
[9] E. Noviana, C.S. Henry, Simultaneous electrochemical detection in paper-based analytical devices, Curr. Opin. Electrochem. 23 (2020) 1–6, https://doi.org/10.1016/j.coelec.2020.02.013.
[10] E. Noviana, T. Ozer, C.S. Carrell, J.S. Link, C. McMahon, I. Jang, C.S. Henry, Microfluidic paper-based analytical devices: from design to applications, Chem. Rev. 121 (2021) 11835–11885, https://doi.org/10.1021/acs.chemrev.0c01335.
[11] V. Caratelli, E. Di Meo, N. Colozza, L. Fabiani, L. Fiore, D. Moscone, F. Arduini, Nanomaterials and paper-based electrochemical devices: merging strategies for fostering sustainable detection of biomarkers, J. Mater. Chem. B 10 (2022) 9021–9039, https://doi.org/10.1039/D2TB00387B.
[12] N. Colozza, V. Caratelli, D. Moscone, F. Arduini, Origami paper-based electrochemical (bio)sensors: state of the art and perspective, Biosensors. 11 (2021) 328, https://doi.org/10.3390/bios11090328.
[13] N. Colozza, V. Caratelli, D. Moscone, F. Arduini, Paper-based devices as new smart analytical tools for sustainable detection of environmental pollutants, Case Stud. Chem. Environ. Eng. 4 (2021), 100167, https://doi.org/10.1016/j.cscee.2021.100167.
[14] V. Borse, P. Chandra, R. Srivastava, BioSensing, Theranostics, and Medical Devices 2.3.1.2, Springer, Singapore, 2022.
[15] A.W. Martinez, S.T. Phillips, E. Carrilho, S.W. Thomas, H. Sindi, G.M. Whitesides, Simple telemedicine for developing regions: camera phones and paper-based microfluidic devices for real-time, off-site diagnosis, Anal. Chem. 80 (2008) 3699–3707, https://doi.org/10.1021/ac800112r.
[16] W. Dungchai, O. Chailapakul, C.S. Henry, Electrochemical detection for paper-based microfluidics, Anal. Chem. 81 (2009) 5821–5826, https://doi.org/10.1021/ac9007573.
[17] W. Mazurkiewicz, M. Podrażka, E. Jarosińska, K. Kappalakandy Valapil, M. Wiloch, M. Jönsson-Niedziółka, E. Witkowska Nery, Paper-based electrochemical sensors and how to make them (work), ChemElectroChem 7 (2020) 2939–2956, https://doi.org/10.1002/celc.202000512.
[18] C. Dincer, R. Bruch, E. Costa-Rama, M.T. Fernández-Abedul, A. Merkoçi, A. Manz, G.A. Urban, F. Güder, Disposable sensors in diagnostics, food, and environmental monitoring, Adv. Mater. (2019) 1806739, https://doi.org/10.1002/adma.201806739.
[19] J. Banks, J. Watt, On a new method of preparing a test liquor to shew the presence of acids and alkalies in chemical mixtures, Phil. Trans. R. Soc. 74 (1784) 419–422, https://doi.org/10.1098/rstl.1784.0031.
[20] M. Baharfar, M. Rahbar, M. Tajik, Engineering strategies for enhancing the performance of electrochemical paper-based analytical devices, Biosens. Bioelectron. 167 (2020), 112506, https://doi.org/10.1016/j.bios.2020.112506.
[21] P. Chandra, K. Mahato (Eds.), Miniaturized biosensing devices: fabrication and applications 2.7.2, Springer Nature, 2022.
[22] M. González del Campo, A. Vaquer, R. de la Rica, Polymer Components for Paper-Based Analytical Devices, Advanced Materials Technologies 7 (2022), 2200140, https://doi.org/10.1002/admt.202200140.
[23] A.K. Yetisen, M.S. Akram, C.R. Lowe, Paper-based microfluidic point-of-care diagnostic devices, Lab Chip 13 (2013) 2210, https://doi.org/10.1039/c3lc50169h.
[24] Y. Habibi, Key advances in the chemical modification of nanocelluloses, Chem. Soc. Rev. 43 (2014) 1519–1542, https://doi.org/10.1039/C3CS60204D.
[25] D. Klemm, B. Heublein, H. Fink, A. Bohn, Cellulose: fascinating biopolymer and sustainable raw material, Angew. Chem. Int. Ed. 44 (2005) 3358–3393, https://doi.org/10.1002/anie.200460587.
[26] E. Princi, S. Vicini, Graft polymerisation of ethyl acrylate/methyl methacrylate copolymers: a tool for the consolidation of paper-based materials, Eur. Polym. J. 44 (2008) 2392–2403, https://doi.org/10.1016/j.eurpolymj.2008.05.008.
[27] R. Bongiovanni, E. Zeno, A. Pollicino, P.M. Serafini, C. Tonelli, UV light-induced grafting of fluorinated monomer onto cellulose sheets, Cellulose 18 (2011) 117–126, https://doi.org/10.1007/s10570-010-9451-5.
[28] E.W. Nery, L.T. Kubota, Sensing approaches on paper-based devices: a review, Anal. Bioanal. Chem. 405 (2013) 7573–7595, https://doi.org/10.1007/s00216-013-6911-4.
[29] R. Ray, A. Prabhu, D. Prasad, V.K. Garlapati, T.M. Aminabhavi, N.K. Mani, J. Simal-Gandara, Paper-based microfluidic devices for food adulterants: cost-effective technological monitoring systems, Food Chem. 390 (2022), 133173, https://doi.org/10.1016/j.foodchem.2022.133173.
[30] R.H. Tang, L.N. Liu, S.F. Zhang, X.C. He, X.J. Li, F. Xu, Y.H. Ni, F. Li, A review on advances in methods for modification of paper supports for use in point-of-care testing, Microchim Acta. 186 (2019) 521, https://doi.org/10.1007/s00604-019-3626-z.
[31] F. Li, M. You, S. Li, J. Hu, C. Liu, Y. Gong, H. Yang, F. Xu, Paper-based point-of-care immunoassays: recent advances and emerging trends, Biotechnol. Adv. 39 (2020), 107442, https://doi.org/10.1016/j.biotechadv.2019.107442.
[32] S.M. Zakir Hossain, Roger E. Luckham, Meghan J. McFadden, et al., Reagentless bidirectional lateral flow bioactive paper sensors for detection of pesticides in beverage and food samples, Anal. Chem. 81 (21) (2009) 9055–9064.
[33] W.R. De Araujo, T.R.L.C. Paixão, Fabrication of disposable electrochemical devices using silver ink and office paper, Analyst 139 (2014) 2742–2747, https://doi.org/10.1039/C4AN00097H.
[34] A. Arena, N. Donato, G. Saitta, A. Bonavita, G. Rizzo, G. Neri, Flexible ethanol sensors on glossy paper substrates operating at room temperature, Sens. Actuators B 145 (2010) 488–494, https://doi.org/10.1016/j.snb.2009.12.053.
[35] T. Ozer, C. McMahon, C.S. Henry, Advances in paper-based analytical devices, annual, Rev. Anal. Chem. 13 (2020) 85–109, https://doi.org/10.1146/annurev-anchem-061318-114845.
[36] T.R. de Oliveira, W.T. Fonseca, G. de Oliveira Setti, R.C. Faria, Fast and flexible strategy to produce electrochemical paper-based analytical devices using a craft cutter printer to create wax barrier and screen-printed electrodes, Talanta 195 (2019) 480–489, https://doi.org/10.1016/j.talanta.2018.11.047.
[37] X. Weng, Z. Fu, C. Zhang, W. Jiang, H. Jiang, A portable 3D microfluidic origami biosensor for cortisol detection in human sweat, Anal. Chem. 94 (2022) 3526–3534, https://doi.org/10.1021/acs.analchem.1c04508.
[38] Y.K. Oh, H. Joung, S. Kim, M. Kim, Vertical flow immunoassay (VFA) biosensor for a rapid one-step immunoassay, Lab on a Chip 13 (2013) 768–772, https://doi.org/10.1039/C2LC41016H.

[39] W. Li, D. Qian, Q. Wang, Y. Li, N. Bao, H. Gu, C. Yu, Fully-drawn origami paper analytical device for electrochemical detection of glucose, Sens. Actuators B 231 (2016) 230–238, https://doi.org/10.1016/j.snb.2016.03.031.
[40] B. Liang, Q. Zhu, L. Fang, Q. Cao, X. Liang, X. Ye, An origami paper device for complete elimination of interferents in enzymatic electrochemical biosensors, Electrochem. Commun. 82 (2017) 43–46, https://doi.org/10.1016/j.elecom.2017.07.001.
[41] S. Cinti, R. Cusenza, D. Moscone, F. Arduini, Paper-based synthesis of Prussian blue nanoparticles for the development of whole blood glucose electrochemical biosensor, Talanta. 187 (2018) 59–64, https://doi.org/10.1016/j.talanta.2018.05.015.
[42] L. Fiore, A. Sinha, N. Seddaoui, J. Di Biasio, F. Ricci, G.M. Stojanovic, F. Arduini, Paper card-like electrochemical platform as a smart point-of-care device for reagent-free glucose measurement in tears, Chem. Commun. 59 (2023) 4300–4303, https://doi.org/10.1039/D2CC06561D.
[43] S. Cinti, F. Arduini, G. Vellucci, I. Cacciotti, F. Nanni, D. Moscone, Carbon black assisted tailoring of Prussian blue nanoparticles to tune sensitivity and detection limit towards H 2 O 2 by using screen-printed electrode, Electrochem. Commun. 47 (2014) 63–66, https://doi.org/10.1016/j.elecom.2014.07.018.
[44] S. Cinti, M. Basso, D. Moscone, F. Arduini, A paper-based nanomodified electrochemical biosensor for ethanol detection in beers, Anal. Chim. Acta 960 (2017) 123–130, https://doi.org/10.1016/j.aca.2017.01.010.
[45] S. Cinti, C. Minotti, D. Moscone, G. Palleschi, F. Arduini, Fully integrated ready-to-use paper-based electrochemical biosensor to detect nerve agents, Biosens. Bioelectron. 93 (2017) 46–51, https://doi.org/10.1016/j.bios.2016.10.091.
[46] A. Cioffi, M. Mancini, V. Gioia, S. Cinti, Office paper-based electrochemical strips for organophosphorus pesticide monitoring in agricultural soil, Environ. Sci. Technol. 55 (2021) 8859–8865, https://doi.org/10.1021/acs.est.1c01931.
[47] J. Ding, B. Li, L. Chen, W. Qin, A three-dimensional origami paper-based device for potentiometric biosensing, Angew. Chem. Int. Ed. 55 (2016) 13033–13037, https://doi.org/10.1002/anie.201606268.
[48] F. Arduini, S. Cinti, V. Caratelli, L. Amendola, G. Palleschi, D. Moscone, Origami multiple paper-based electrochemical biosensors for pesticide detection, Biosens. Bioelectron. 126 (2019) 346–354, https://doi.org/10.1016/j.bios.2018.10.014.
[49] V. Caratelli, G. Fegatelli, D. Moscone, F. Arduini, A paper-based electrochemical device for the detection of pesticides in aerosol phase inspired by nature: a flower-like origami biosensor for precision agriculture, Biosens. Bioelectron. 205 (2022), 114119, https://doi.org/10.1016/j.bios.2022.114119.
[50] N. Colozza, K. Kehe, G. Dionisi, T. Popp, A. Tsoutsoulopoulos, D. Steinritz, D. Moscone, F. Arduini, A wearable origami-like paper-based electrochemical biosensor for sulfur mustard detection, Biosens. Bioelectron. 129 (2019) 15–23, https://doi.org/10.1016/j.bios.2019.01.002.
[51] C.-C. Wang, J.W. Hennek, A. Ainla, A.A. Kumar, W.-J. Lan, J. Im, B.S. Smith, M. Zhao, G.M. Whitesides, A. Paper-Based, "Pop-up" electrochemical device for analysis of beta-hydroxybutyrate, Anal. Chem. 88 (2016) 6326–6333, https://doi.org/10.1021/acs.analchem.6b00568.
[52] C.M. Moreira, S.V. Pereira, J. Raba, F.A. Bertolino, G.A. Messina, Paper-based enzymatic platform coupled to screen printed graphene-modified electrode for the fast neonatal screening of phenylketonuria, Clin. Chim. Acta 486 (2018) 59–65, https://doi.org/10.1016/j.cca.2018.07.016.
[53] M. Li, L. Wang, R. Liu, J. Li, Q. Zhang, G. Shi, Y. Li, C. Hou, H. Wang, A highly integrated sensing paper for wearable electrochemical sweat analysis, Biosens. Bioelectron. 174 (2021), 112828, https://doi.org/10.1016/j.bios.2020.112828.
[54] E.L. Fava, T.A. Silva, T.M.D. Prado, F.C.D. Moraes, R.C. Faria, O. Fatibello-Filho, Electrochemical paper-based microfluidic device for high throughput multiplexed analysis, Talanta. 203 (2019) 280–286, https://doi.org/10.1016/j.talanta.2019.05.081.
[55] E.S. Ribeiro, B.S. De Farias, T.R. Sant'Anna Cadaval Junior, L.A. De Almeida Pinto, P.S. Diaz, Chitosan–based nanofibers for enzyme immobilization, Int. J. Biol. Macromol. 183 (2021) 1959–1970, https://doi.org/10.1016/j.ijbiomac.2021.05.214.
[56] F.H. Cincotto, E.L. Fava, F.C. Moraes, O. Fatibello-Filho, R.C. Faria, A new disposable microfluidic electrochemical paper-based device for the simultaneous determination of clinical biomarkers, Talanta. 195 (2019) 62–68, https://doi.org/10.1016/j.talanta.2018.11.022.
[57] L. Cao, G.-C. Han, H. Xiao, Z. Chen, C. Fang, A novel 3D paper-based microfluidic electrochemical glucose biosensor based on rGO-TEPA/PB sensitive film, Anal. Chim. Acta 1096 (2020) 34–43, https://doi.org/10.1016/j.aca.2019.10.049.
[58] P. Chandra, R. Prakash, Nanobiomaterial Engineering vol. 10, Springer, Singapore, 2020, p. 2.
[59] X. Ruan, Y. Wang, E.Y. Kwon, L. Wang, N. Cheng, X. Niu, S. Ding, B.J. Van Wie, Y. Lin, D. Du, Nanomaterial-enhanced 3D-printed sensor platform for simultaneous detection of atrazine and acetochlor, Biosens. Bioelectron. 184 (2021), 113238, https://doi.org/10.1016/j.bios.2021.113238.
[60] J. Bhardwaj, A. Sharma, J. Jang, Vertical flow-based paper immunosensor for rapid electrochemical and colorimetric detection of influenza virus using a different pore size sample pad, Biosens. Bioelectron. 126 (2019) 36–43, https://doi.org/10.1016/j.bios.2018.10.008.
[61] I.C. Samper, A. Sánchez-Cano, W. Khamcharoen, I. Jang, W. Siangproh, E. Baldrich, B.J. Geiss, D.S. Dandy, C.S. Henry, Electrochemical capillary-flow immunoassay for detecting anti-SARS-CoV-2 Nucleocapsid protein antibodies at the point of care, ACS Sens. 6 (2021) 4067–4075, https://doi.org/10.1021/acssensors.1c01527.
[62] S. Boonkaew, S. Chaiyo, S. Jampasa, S. Rengpipat, W. Siangproh, O. Chailapakul, An origami paper-based electrochemical immunoassay for the C-reactive protein using a screen-printed carbon electrode modified with graphene and gold nanoparticles, Microchim. Acta 186 (2019) 153, https://doi.org/10.1007/s00604-019-3245-8.
[63] M. Pavithra, S. Muruganand, C. Parthiban, Development of novel paper based electrochemical immunosensor with self-made gold nanoparticle ink and quinone derivate for highly sensitive carcinoembryonic antigen, Sens. Actuators B 257 (2018) 496–503, https://doi.org/10.1016/j.snb.2017.10.177.
[64] Y. Wang, H. Xu, J. Luo, J. Liu, L. Wang, Y. Fan, S. Yan, Y. Yang, X. Cai, A novel label-free microfluidic paper-based immunosensor for highly sensitive electrochemical detection of carcinoembryonic antigen, Biosens. Bioelectron. 83 (2016) 319–326, https://doi.org/10.1016/j.bios.2016.04.062.
[65] Y. Wang, J. Luo, J. Liu, X. Li, Z. Kong, H. Jin, X. Cai, Electrochemical integrated paper-based immunosensor modified with multi-walled carbon nanotubes nanocomposites for point-of-care testing of 17β-estradiol, Biosens. Bioelectron. 107 (2018) 47–53, https://doi.org/10.1016/j.bios.2018.02.012.
[66] G. Sun, L. Zhang, Y. Zhang, H. Yang, C. Ma, S. Ge, M. Yan, J. Yu, X. Song, Multiplexed enzyme-free electrochemical immunosensor based on ZnO nanorods modified reduced graphene oxide-paper electrode and silver deposition-induced signal amplification strategy, Biosens. Bioelectron. 71 (2015) 30–36, https://doi.org/10.1016/j.bios.2015.04.007.
[67] Daesoon Lee, Jyoti Bhardwaj, Jaesung Jang, Based electrochemical immunosensor for label-free detection of multiple avian influenza virus antigens using flexible screen-printed carbon nanotube-polydimethylsiloxane electrodes, Sci. Rep. 12 (1) (2022) 2311.
[68] P. Pusomjit, P. Teengam, N. Chuaypen, P. Tangkijvanich, N. Thepsuparungsikul, O. Chailapakul, Electrochemical immunoassay for detection of hepatitis C virus core antigen using electrode modified with Pt-decorated single-walled carbon nanotubes, Microchim Acta. 189 (2022) 339, https://doi.org/10.1007/s00604-022-05400-8.
[69] J. Jaewjaroenwattana, W. Phoolcharoen, E. Pasomsub, P. Teengam, O. Chailapakul, Electrochemical paper-based antigen sensing platform using plant-derived monoclonal antibody for detecting SARS-CoV-2, Talanta. 251 (2023), 123783, https://doi.org/10.1016/j.talanta.2022.123783.
[70] M.L. Scala-Benuzzi, J. Raba, G.J.A.A. Soler-Illia, R.J. Schneider, G.A. Messina, Novel electrochemical paper-based immunocapture assay for the quantitative determination of ethinylestradiol in water samples, Anal. Chem. 90 (2018) 4104–4111, https://doi.org/10.1021/acs.analchem.8b00028.
[71] A. Lamaoui, A. Karrat, A. Amine, Molecularly imprinted polymer integrated into paper-based analytical device for smartphone-based detection: application for sulfamethoxazole, Sens. Actuators B 368 (2022), 132122, https://doi.org/10.1016/j.snb.2022.132122.
[72] L. Ge, S. Wang, J. Yu, N. Li, S. Ge, M. Yan, Molecularly imprinted polymer grafted porous Au-paper electrode for an microfluidic electro-analytical origami device, Adv. Funct. Mater. 23 (2013) 3115–3123, https://doi.org/10.1002/adfm.201202785.
[73] X. Sun, Y. Jian, H. Wang, S. Ge, M. Yan, J. Yu, Ultrasensitive microfluidic paper-based electrochemical biosensor based on molecularly imprinted film and Boronate affinity sandwich assay for glycoprotein detection, ACS Appl. Mater. Interfaces 11 (2019) 16198–16206, https://doi.org/10.1021/acsami.9b02005.
[74] M. Amatatongchai, J. Sitanurak, W. Sroysee, S. Sodanat, S. Chairam, P. Jarujamrus, D. Nacapricha, P.A. Lieberzeit, Highly sensitive and selective electrochemical paper-based device using a graphite screen-printed electrode modified with molecularly imprinted polymers coated Fe3O4@Au@SiO2 for serotonin determination, Anal. Chim. Acta 1077 (2019) 255–265, https://doi.org/10.1016/j.aca.2019.05.047.
[75] P. Sodkrathok, C. Karuwan, W. Kamsong, A. Tuantranont, M. Amatatongchai, Patulin-imprinted origami 3D-ePAD based on graphene screen-printed electrode modified with Mn–ZnS quantum dot coated with a molecularly imprinted polymer, Talanta. 262 (2023), 124695, https://doi.org/10.1016/j.talanta.2023.124695.
[76] N. Nontawong, P. Ngaosri, S. Chunta, P. Jarujamrus, D. Nacapricha, P. A. Lieberzeit, M. Amatatongchai, Smart sensor for assessment of oxidative/nitrative stress biomarkers using a dual-imprinted electrochemical paper-based analytical device, Anal. Chim. Acta 1191 (2022), 339363, https://doi.org/10.1016/j.aca.2021.339363.
[77] M. Amatatongchai, N. Nontawong, P. Ngaosri, S. Chunta, S. Wanram, P. Jarujamrus, D. Nacapricha, P.A. Lieberzeit, Facile and compact electrochemical paper-based analytical device for point-of-care diagnostic of dual carcinogen oxidative stress biomarkers through a molecularly imprinted polymer coated on graphene quantum-dot capped gold, Anal. Chem. 94 (2022) 16692–16700, https://doi.org/10.1021/acs.analchem.2c03120.
[78] S. Cinti, G. Cinotti, C. Parolo, E.P. Nguyen, V. Caratelli, D. Moscone, F. Arduini, A. Merkoci, Experimental comparison in sensing breast cancer mutations by signal ON and signal OFF paper-based electroanalytical strips, Anal. Chem. 92 (2020) 1674–1679, https://doi.org/10.1021/acs.analchem.9b02560.
[79] Y. Liu, K. Cui, Q. Kong, L. Zhang, S. Ge, J. Yu, A self-powered origami paper analytical device with a pop-up structure for dual-mode electrochemical sensing of ATP assisted by glucose oxidase-triggered reaction, Biosens. Bioelectron. 148 (2020), 111839, https://doi.org/10.1016/j.bios.2019.111839.
[80] Q. Lu, T. Su, Z. Shang, D. Jin, Y. Shu, Q. Xu, X. Hu, Flexible paper-based Ni-MOF composite/AuNPs/CNTs film electrode for HIV DNA detection, Biosens. Bioelectron. 184 (2021), 113229, https://doi.org/10.1016/j.bios.2021.113229.
[81] P.E. Nielsen, M. Egholm, R.H. Berg, O. Buchardt, Sequence-selective recognition of DNA by Strand displacement with a thymine-substituted polyamide, Science. 254 (1991) 1497–1500, https://doi.org/10.1126/science.1962210.
[82] T. Vilaivan, C. Srisuwannaket, Hybridization of pyrrolidinyl peptide nucleic acids and DNA: selectivity, base-pairing specificity, and direction of binding, Org. Lett. 8 (2006) 1897–1900, https://doi.org/10.1021/ol060448q.

[83] P. Teengam, W. Siangproh, A. Tuantranont, C.S. Henry, T. Vilaivan, O. Chailapakul, Electrochemical paper-based peptide nucleic acid biosensor for detecting human papillomavirus, Anal. Chim. Acta 952 (2017) 32–40, https://doi.org/10.1016/j.aca.2016.11.071.
[84] P. Teengam, W. Siangproh, A. Tuantranont, T. Vilaivan, O. Chailapakul, C. S. Henry, Electrochemical impedance-based DNA sensor using pyrrolidinyl peptide nucleic acids for tuberculosis detection, Anal. Chim. Acta 1044 (2018) 102–109, https://doi.org/10.1016/j.aca.2018.07.045.
[85] A. Lomae, P. Preechakasedkit, O. Hanpanich, T. Ozer, C.S. Henry, A. Maruyama, E. Pasomsub, A. Phuphuakrat, S. Rengpipat, T. Vilaivan, O. Chailapakul, N. Ruecha, N. Ngamrojanavanich, Label free electrochemical DNA biosensor for COVID-19 diagnosis, Talanta. 253 (2023), 123992, https://doi.org/10.1016/j.talanta.2022.123992.
[86] C. Srisomwat, A. Yakoh, N. Chuaypen, P. Tangkijvanich, T. Vilaivan, O. Chailapakul, Amplification-free DNA sensor for the one-step detection of the hepatitis B virus using an automated paper-based lateral flow electrochemical device, Anal. Chem. 93 (2021) 2879–2887, https://doi.org/10.1021/acs.analchem.0c04283.
[87] M.A. Morales, J.M. Halpern, Guide to selecting a biorecognition element for biosensors, Bioconjug. Chem. 29 (2018) 3231–3239, https://doi.org/10.1021/acs.bioconjchem.8b00592.
[88] H. Liu, Y. Xiang, Y. Lu, R.M. Crooks, Aptamer-based origami paper analytical device for electrochemical detection of adenosine, Angew. Chem. Int. Ed. 51 (2012) 6925–6928, https://doi.org/10.1002/anie.201202929.
[89] H. Jiang, Q. Guo, C. Zhang, Z. Sun, X. Weng, Microfluidic origami nano-aptasensor for peanut allergen Ara h1 detection, Food Chem. 365 (2021), 130511, https://doi.org/10.1016/j.foodchem.2021.130511.
[90] M. Su, L. Ge, S. Ge, N. Li, J. Yu, M. Yan, J. Huang, Paper-based electrochemical cyto-device for sensitive detection of cancer cells and in situ anticancer drug screening, Anal. Chim. Acta 847 (2014) 1–9, https://doi.org/10.1016/j.aca.2014.08.013.
[91] B. Wei, K. Mao, N. Liu, M. Zhang, Z. Yang, Graphene nanocomposites modified electrochemical aptamer sensor for rapid and highly sensitive detection of prostate specific antigen, Biosens. Bioelectron. 121 (2018) 41–46, https://doi.org/10.1016/j.bios.2018.08.067.
[92] Y. Xing, J. Liu, S. Sun, T. Ming, Y. Wang, J. Luo, G. Xiao, X. Li, J. Xie, X. Cai, New electrochemical method for programmed death-ligand 1 detection based on a paper-based microfluidic aptasensor, Bioelectrochemistry. 140 (2021), 107789, https://doi.org/10.1016/j.bioelechem.2021.107789.
[93] T. Ming, Y. Cheng, Y. Xing, J. Luo, G. Mao, J. Liu, S. Sun, F. Kong, H. Jin, X. Cai, Electrochemical microfluidic paper-based aptasensor platform based on a biotin–streptavidin system for label-free detection of biomarkers, ACS Appl. Mater. Interfaces 13 (2021) 46317–46324, https://doi.org/10.1021/acsami.1c12716.
[94] Y. Wang, J. Luo, J. Liu, S. Sun, Y. Xiong, Y. Ma, S. Yan, Y. Yang, H. Yin, X. Cai, Label-free microfluidic paper-based electrochemical aptasensor for ultrasensitive and simultaneous multiplexed detection of cancer biomarkers, Biosens. Bioelectron. 136 (2019) 84–90, https://doi.org/10.1016/j.bios.2019.04.032.
[95] S. Ge, L. Zhang, Y. Zhang, H. Liu, J. Huang, M. Yan, J. Yu, Electrochemical K-562 cells sensor based on origami paper device for point-of-care testing, Talanta. 145 (2015) 12–19, https://doi.org/10.1016/j.talanta.2015.05.008.
[96] V. Caratelli, S. Fillo, N. D'Amore, O. Rossetto, M. Pirazzini, M. Moccia, C. Avitabile, D. Moscone, F. Lista, F. Arduini, Paper-based electrochemical peptide sensor for on-site detection of botulinum neurotoxin serotype A and C, Biosens. Bioelectron. 183 (2021), 113210, https://doi.org/10.1016/j.bios.2021.113210.
[97] S. Cinti, F. Arduini, Graphene-based screen-printed electrochemical (bio) sensors and their applications: efforts and criticisms, Biosens. Bioelectron. 89 (2017) 107–122, https://doi.org/10.1016/j.bios.2016.07.005.